

See discussions, stats, and author profiles for this publication at: <https://www.researchgate.net/publication/313864185>

Wearable and Miniaturized Sensor Technologies for Personalized and Preventive Medicine

Article in *Advanced Functional Materials* · February 2017

DOI: 10.1002/adfm.201605271

CITATIONS

167

READS

3,896

3 authors, including:



Antonio Tricoli

The University of Sydney

198 PUBLICATIONS 4,655 CITATIONS

SEE PROFILE



Noushin Nasiri

Macquarie University

55 PUBLICATIONS 1,065 CITATIONS

SEE PROFILE

Some of the authors of this publication are also working on these related projects:



Thin Films and Nanotechnology [View project](#)



Ethylene gas sensing [View project](#)

Wearable and Miniaturized Sensor Technologies for Personalized and Preventive Medicine

Antonio Tricoli,* Noushin Nasiri, and Sayan De

The unprecedented medical achievements of the last century have dramatically improved our quality of life. Today, the high cost of many healthcare approaches challenges their long-term financial sustainability and translation to a global scale. The convergence of wearable electronics, miniaturized sensor technologies, and big data analysis provides novel opportunities to improve the quality of healthcare while decreasing costs by the very early stage detection and prevention of fatal and chronic diseases. Here, some exciting achievements, emerging technologies, and standing challenges for the development of non-invasive personalized and preventive medicine devices are discussed. The engineering of wire- and power-less ultra-thin sensors on wearable biocompatible materials that can be placed on the skin, pupil, and teeth is reviewed, focusing on common solutions and current limitations. The integration and development of sophisticated sensing nanomaterials are presented with respect to their performance, showing exemplary implementations for the detection of ultra-low concentrations of biomarkers in complex mixtures such as the human sweat and breath. This review is concluded by summarizing achievements and standing challenges with the aim to provide directions for future research in miniaturized medical sensor technologies.

1. Introduction

The unprecedented technological and economic achievements of the last century have had numerous and profound impacts on our quality of life and lifestyle. Amongst the most remarkable, life expectancy at birth has climbed from less than 50 years at the start of the 20th century to more than 80 years in many developed countries today.^[1] This 60% increase in life expectancy has been driven by several factors, including food security, large-scale production of essential drugs such as antibiotics, and the development of novel medical technologies and procedures such as computed tomography, magnetic resonance, and keyhole surgery.^[2] This technological drive does not seem to be losing its momentum, and once undreamed-of possibilities such as the engineering of synthetic replicas of

organs by 3D printing of anatomically and functionally equivalent copies are rapidly approaching commercial maturity.^[3] The translation of these successes on a global scale has been proven challenging, and many developing countries still have life expectancies of 50–60 years.^[1] Amongst others, a major challenge is the high cost of modern medicine approaches. Recent OECD data^[1] show a quasi-asymptotic correlation between life expectancy at birth and annual per capita healthcare spending, with an annual average expenditure of ca. 2000 USD per capita being the 2015 threshold for countries having an average life expectancy at birth of 80 years or more.^[1] Even by developed countries' standards, this is a large sum, and healthcare expenditures are a major budget item of many countries, reaching ca. 10% of the gross domestic product (GDP) in many of them, and peaking to 17% of the GDP in the United States of America.^[1] The long-term economic sustainability of most developed medical systems is fragile, and

many European states are forced by their increasing public debt to consider cuts to their healthcare expenditures. In addition, novel risk factors such as the rise of antibiotic-resistant superbugs and anthropogenic diseases undermine our future reliance on established medical praxis.

An opportunity to decrease overall costs of healthcare services while improving their quality is given by preventive and personalized medicine approaches. Very-early-stage medical diagnostics can significantly increase the chances of successfully treating widespread diseases such as lung cancer and melanoma, while decreasing the overall treatment costs. Recurrent monitoring of important biomarkers and taking corrective actions can help prevent the development of chronic illnesses such as asthma and circulatory system disorders. While such large-scale screenings are helping to fight against severe diseases such as prostate and breast cancer, the relatively high cost of many medical diagnostics approaches does not allow using similar screening approaches for many other diseases. A paradigm shift may be offered by the convergence of novel wearable electronic technologies and big data analysis methodologies. Several life-style and health monitoring devices, with exemplary cases being the Fitbit^[4] and smart watches,^[5] are already commercially available. While initial application of these wearable electronics was centered on the monitoring of an individual's

Prof. A. Tricoli, N. Nasiri, S. De
Nanotechnology Research Laboratory
Research School of Engineering
Australian National University
Canberra 2601, Australia
E-mail: antonio.tricoli@anu.edu.au



DOI: 10.1002/adfm.201605271

data, it is becoming rapidly apparent that their added value may consist in drawing large-scale correlations from the pattern analysis of millions of users. With the right set of measurable metabolic indicators, this concept has the potential to revolutionize our understanding of many difficult-to-cure diseases, and provide new ways for their prevention and very early stage minimalistic treatment.

The development of miniaturized and wearable devices for personalized and preventive medicine is driving a renaissance in sensor and analytical chemistry research.^[6] Efforts are shifting from more traditional chemical and process engineering to the biotechnology and commercial electronic industries. These bring new challenges and constraints, such as a requirement for miniaturized devices of a few millimeters in size that can be integrated in on-chip electronic systems with ultra-low power consumption. Transmission and collection of the data is also not a trivial undertaking, as the non-invasive nature of these approaches often requires their physical connection to difficult-to-reach areas, such as the iris of the eye and the mouth. Integrated passive wireless data transmission systems are becoming a key component for the next generation of wearable devices. Requirements for the sensing systems are even more demanding, as the implementation of bulky analytical approaches such as chromatography and mass spectrometry is hardly achievable on a millimeter scale.

Quasi- and full-solid-state sensing technologies are emerging as a highly miniaturizable solution for the accurate measurement of trace concentrations of biomarkers and other metabolic indicators.^[7] Sophisticated microscale architectures are being demonstrated thanks to the rapid progress of microfabrication approaches.^[8] Nanotechnology has become essential to impart sufficient sensitivity to the detector surface for biomarker detection, demonstrating a thousand-fold increase in the lower limit of detection and new opportunities to increase selectivity while decreasing power consumption.^[9] Early work on non-invasive diabetes diagnostics has demonstrated that this is possible by breath analysis.^[10] Simple solid-state devices made of unique nanomaterial compositions can sense acetone, the primary breath marker for diabetes, in the human breath down to a few particles per billion. Nanostructuring and functionalization of electrochemical micro-electrodes on flexible polymer lenses is enabling the online measurement of glucose and other key biomarkers directly from human tears.^[11] Swallowable gas sensing capsules are being developed to measure key gas molecules in the digestive system, providing unique new insights in metabolic processes and disorders.^[12] A significant effort is being spent in extending these successful sensor engineering approaches to a larger group of biomarkers. This is not an easy task, as differentiating between the thousands of molecules present in body fluids such as tears, sweat, and saliva, and exhaled through the skin and breath, requires atomic-scale tailoring of reaction sites and efficient transduction of sensing reactions.

Here, we aim to present some of the ongoing key innovations in materials science and micro/nano-fabrication technologies that are setting the basis for future preventive and personalized medicine devices and approaches. We will discuss the challenges and emerging solutions associated with the engineering of wearable and miniaturized sensors for the continuous non-invasive monitoring of biomarkers from readily available



Mechanical and Process Engineering and in 2010 his PhD in Nanotechnology.

Antonio Tricoli is the head of the Nanotechnology Research Laboratory, established in 2012, at the Australian National University. His group focuses on the multi-scale engineering of nanomaterials and devices for emerging medical and energy technologies. He pursued his studies at ETH Zurich, where he received his diploma in



She submitted her PhD thesis in 2016 on the engineering of optoelectronic devices by gas-phase nanofabrication approaches.

Noushin Nasiri received her Masters of Engineering in Materials Engineering from the University of Tehran in Iran in 2010. She continued her research as a research assistant at the University of Tehran for two years and started her PhD in 2012 at the Nanotechnology Research Laboratory of the Australian National University (ANU).



semiconductors for the monitoring and diagnosis of diabetes mellitus.

Sayan De completed his honors degree in Biomedical Engineering in 2016 at the Australian National University. He is a member of the Nanotechnology Research Laboratory under the supervision of Associate Professor Antonio Tricoli. His research thesis focused on the development of tailored gas-sensing

pathways such as sweat, tears, and breath. We will critically compare some of the most recent and exciting miniaturized devices for non-invasive medical diagnostics, focusing on the recent achievements in wireless sensing, ultra-low power consumption, and flexible electronics. We will conclude this review by pointing to existing challenges that the research and industrial community is facing in trying to extend these successful examples to a broader spectrum of essential biomarkers and related devices, aiming to provide solid guidelines for future research directions and studies.

2. Classification of Emerging Miniaturized and Wearable Sensing Technologies

A classification of emerging sensing technologies can be attempted according to their sensing mechanism and application. While several hybrid systems are being proposed that challenge the establishment of rigid categories, common technological solutions are often found as a function of the target analyte. Here, we classify these emerging technologies across two main categories, namely, body fluid sensors and volatile bio-marker analyzers. **Figure 1** shows a schematic summary of some rapidly emerging sensing concepts for personalized and preventive medicine. Several types of miniaturized and wearable devices are being developed for the measurement of key biomarkers without the need of invasive procedures. A major distinction can be made between contact approaches such as tear, sweat, and saliva analysis, and contactless technologies such as breath and perspiration sensors. An additional category includes pressure and optical sensors. A main distinction is that the first two categories require the chemical interaction of a detector with liquid and gas molecules, respectively, while the third relies on the detection of physical signals such as light and pressure. Here, we only discuss the first two categories, that is, body fluid and volatile biomarker analyzers, as they present numerous similarities.

Body fluid sensors are one of the most established tools for miniaturized diagnostics, as large swaths of patients report to doctors daily to test their blood and urine. The typical treatment cycle for diabetes involves drawing blood from the tips of the fingers with a lancet prick, and testing the blood for glucose content.^[19] Pressure sensing is a routine undertaking, with cuff-on-arm blood pressure monitors common during medical check-ups, and take-home devices for patients with ongoing blood pressure concerns.^[20] A major focus is placed on translating current approaches from body fluids that require invasive sampling to non-invasive ones that are more easily available, like sweat.^[21] In contrast, analysis of volatile biomarkers has been driven by recent advances in the characterization of the breath composition.^[22] In fact, although there is a rich history of an understanding between components of the breath and their reflection on physical health,^[23] the concentrations of many key biomarkers are very small and have only started to be characterized with the rise of modern analytical technology, such as proton transfer

reaction mass spectrometry (PTR-MS).^[22] Developing miniaturized and wearable sensors that can replicate the selectivity and sensitivity of these bulky lab-scale analytical tools is a primary focus of current research efforts.^[24]

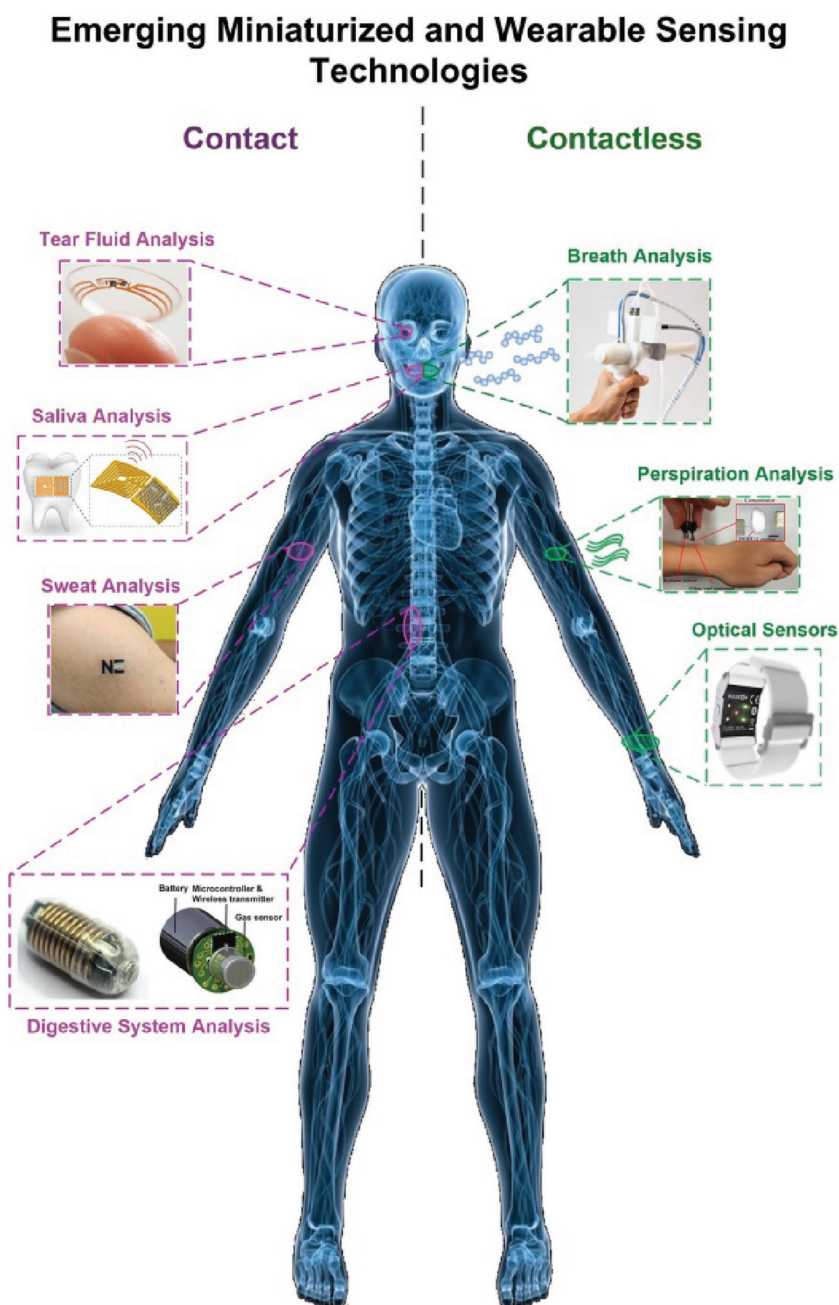


Figure 1. Schematic summary of some emerging sensing technologies for personalized and preventive medicine. A major distinction can be made between contact and contactless technologies, such as tear,^[13b] (Reproduced with permission.^[13b] Copyright 2014, Google X), saliva analysis,^[14] (Reproduced with permission.^[14] Copyright 2012, Nature Publishing Group), sweat,^[15] (Reproduced with permission.^[15] Copyright 2013, American Chemical Society), digestive system^[12] (Reproduced with permission.^[12] Copyright 2016, Elsevier) and optical,^[16] (Reproduced with permission.^[16] Copyright 2015, Institute of Electrical and Electronics Engineers), breath,^[17] (Reproduced with permission.^[17] Copyright 2015, Institute of Physics Publishing) and perspiration sensors.^[18] (Reproduced with permission.^[18] Copyright 2015, American Chemical Society).

3. Body Fluid Biomarkers and Sensors

Commonly targeted body fluids that do not require invasive sampling procedures are tears, sweat, and saliva. A list of common biomarkers measured in these fluids is presented in Table 1. For example, the occurrence of diabetes type II, a chronic systemic disease characterized by raised blood glucose concentration, is steadily increasing, especially in developed countries. Moreover, the treatment of the disease is a major expenditure for modern healthcare systems, with costs expected to rapidly increase even further.^[25] Diabetes can be managed by proper administration of insulin, where correct timing and dosage of the injections are important. Self-monitoring is widely used for controlling the level of glucose in the blood and usually performed by an invasive test, drawing a small amount of blood from the patient and measuring the amount of glucose using a portable glucometer. Nonetheless, this method is not ideal, and development of devices for continuous noninvasive monitoring of blood glucose, such as that possible through the analysis of sweat^[21b,26] and tears,^[11,27] could increase the safety and convenience of testing, leading to improved public health and reduced medical costs.^[28]

More than 1500 proteins are present in human tears.^[27b] Some of these proteins are present in sufficiently high concentrations and can be used for medical purposes. For instance, the observation of antibacterial and antimicrobial function can

be derived from lactoferrin and lysozyme.^[27b] Peptide function can be inferred from the presence of various proteases and protease inhibitors. Information on cholesterol, fatty alcohols, fatty acids, and phospholipids is related to tear lipocalpin, which is one of the major tear proteins.^[27b] Even more valuable, changes in the tear proteome are highly correlated with disorders of the central nervous system (CNS), such as multiple sclerosis.^[29] Problems affecting the CNS are notoriously difficult to diagnose, and the ability to detect them relatively non-invasively from tear fluid may encourage early detection and improve wellness prospects for those affected. In addition, lactate, which can be measured from tears, is an important metabolite in the anaerobic glycolytic pathway in the human body. Under hypoxic conditions, pyruvate is catalytically converted into L-lactate by the enzyme lactate dehydrogenase. Some of the health conditions that cause increased lactate levels are ischemia, which may lead to inadequate tissue oxygenation or insufficient transport of L-lactate to the liver, where most of it is broken down; sepsis and septic shocks; liver diseases; organ failure; stroke; as well as different types of cancer.^[30] It is also a biomarker of tissue oxygenation, information that is useful to athletes. Intense physical activity can nullify the standard metabolism pathways, and causes an anaerobic process to consume glycogen for energy, leading to muscle cells producing lactate. This is known as 'glycolysis' or 'lactate acidosis'. As such, lactate levels in blood are routinely measured

Table 1. List of common biomarkers measured in readily available body fluids.

Fluid	Biomarker	Purpose	Levels	Sensing technology	Ref.
	Caffeine	Metabolizing activity in hepatocytes	6×10^{-6} M	Potentiometric	[34]
	CD59	Oral cancer diagnosis	0.38 fg mL^{-1}	Electrochemical	[35]
	CYFRA-21-1	Oral cancer diagnosis	0.122 ng mL^{-1}	Differential pulse voltammetry	[36]
	Chloride	Kidney disease	300 mg g^{-1}	Chronoamperometry	[37]
			0.003×10^{-3} M	Electrochemical	[38]
Saliva	Glucose	Diabetes	1.1 mg dL^{-1}		[39]
			$5 \text{ } \mu\text{mol L}^{-1}$		[40]
			0.22×10^{-6} M	Electro-chemiluminescence	[41]
	Lactate	Physical exertion	0.5 nmol L^{-1}	Chemiluminescence	[42]
	Lead	Exposure complication	1 ppb	Anodic stripping voltammetry	[43]
	Thiocyanate, nitrite, and nitrate	Detection of inorganic metabolites	$3.1\text{--}4.9 \text{ ng mL}^{-1}$	Capillary electrophoresis	[45]
			83 mg dL^{-1}	Artificial neural networks	[46]
	Glucose	Diabetes	720×10^{-6} M	Dual-enzyme biosensor composed of glucose oxidase (GO ₂) and pistol-like DNAzyme (PLDz)	[47]
Sweat	H ₂ O ₂	Physical exertion	0.5 M	Electrochemical	[48]
	Lactate	Physical exertion	0.1 mmol L^{-1}	Chemiluminescence	[42]
	Lactate/pyruvate	Physical exertion	$0.03 \times 10^{-3}/0.001 \times 10^{-3}$ M	LC ^{a)}	[50]
	MDMA	Drug testing	3.2 ng	GC ^{a)} –MS ^{a)}	[51]
	Plasma L-dopa	Parkinson's disease	5 nmol L^{-1}	LC ^{a)} + Electrochemical	[44]
			$6.1 \text{ } \mu\text{g dL}^{-1}$	Ratiometric sensing with near-infrared photonic crystal	[52]
	Glucose	Diabetes	1.5×10^{-6} M	Amperometry	[53]
Tears	Interleukin-1 α	Detecting pathogenic attack	1.43 pg mL^{-1}	Theranostic lens	[49]
	Lactoferrin	Sjögren's syndrome	3×10^{-9} M	Microfluidic immunoassay	[54]

^{a)}LC = liquid chromatography; GC = gas chromatography; MS = mass spectrometry.

for the diagnosis of diseases as well as monitoring the fitness of athletes.^[30e,31]

The compositions of sweat and blood are osmotically related.^[32] As a result, sweat contains trace amounts of magnesium, zinc, iron, and other metals commonly used for medical diagnostics.^[26a] Biomarkers like Na^+ and Cl^- are also common and natural components of sweat. Their composition can be used to give information about cystic fibrosis.^[33] Along with other electrolytes like potassium and NH_4^+ , controlling the concentration of Na^+ and Cl^- can help combat cramping in athletes.^[21c] The correlations between sweat and blood composition may allow for blood-based diagnosis to move toward sweat-based diagnosis, which would have positive impacts on patient compliance and safety as well as allowing continuous monitoring.

Saliva is a great diagnostic fluid providing an alternative to direct blood analysis via the permeation of blood constituents.^[55] Early work in electrochemical salivary sensors was demonstrated by Graf in the 1960s, measuring pH and fluoride ion levels on a partial denture.^[56] Many of the analytes in saliva are heavily associated with oral and systemic diseases, due to the relatively high amount of interaction between these pathways and the mouth. Uric acid (UA) is the end product of purine metabolism in the human body. An abnormal concentration of UA is a biomarker for various diseases, including hyperuricemia, gout, Lesch-Nyhan syndrome, and renal syndrome.^[57] In addition, higher UA levels implicate a higher future risk of type 2 diabetes.^[58] UA can also be an indicator of physical-stress-induced reactive oxygen species (ROS), acting as a free radical scavenger.^[59] While blood UA measurements require invasive blood collection, salivary uric acid (SUA) measurements could be carried out non-invasively and in a continuous real-time manner. Shibasaki et al.^[60] and Soukup et al.^[61] have found a good correlation of UA blood and saliva levels, demonstrating that this metabolite can be monitored in saliva in a noninvasive way without need for blood sampling. The presence of cell cycle regulatory proteins such as Cyclin D1 and ki67 have been found to correlated with oral cancer,^[62] cortisol,

and metastatic breast cancer,^[63] while the expression of certain miRNAs can help to differentiate between acute lymphoid and acute myeloid leukemia.^[64]

Many non-invasive sensors to measure the concentration of biomarkers in readily available body fluids such as sweat, tears, and saliva are based on miniaturized, planar electrochemical cell technology. **Figure 2a,b** shows a simplified schematic of the working mechanism of these amperometric sensors.^[65] They usually consist of working (WE), counter (CE), and reference (RE) electrodes.^[65] A current between the working and counter electrode is generated by targeted redox reactions between the biomarker and the modified working electrode while the opposite reaction takes place at the counter electrode.^[65,66] This results in the generation of an electrochemical current which, in diluted conditions, is proportional to the concentration of the biomarker.^[67] The surface of the working electrode is usually nanotextured to enhance the available surface for redox of the biomolecules, and thus increasing the signal-to-noise ratio as well as lowering the limit of detection. A major advantage is that the selectivity can be enhanced both by coating the nanotexture with highly selective functional groups such as enzymes, antibodies, and carefully engineered peptides, and by selecting the appropriate voltage potential for activation of the selected reaction. Other types of solid-state sensors for body fluid analysis include resistometric and capacitive devices where the detection of the presence and concentration of a biomarker is measured through the change in resistance^[14] and capacitance,^[62,68] respectively, between a set of functionalized electrodes.

Figure 2d shows a schematic of the operation principle of such electrochemical sensors. Commonly, a constant voltage, sufficiently high to initiate the reduction or oxidation of the analyte, is applied between a working and counter electrode. The working electrode is nanostructured and functionalized with an analyte-specific layer such as enzymes and antibodies, providing a selective surface for the redox of the targeted analyte. This results in the rise of a catalytic current between the working and counter electrode, which is proportional to the analyte concentration.

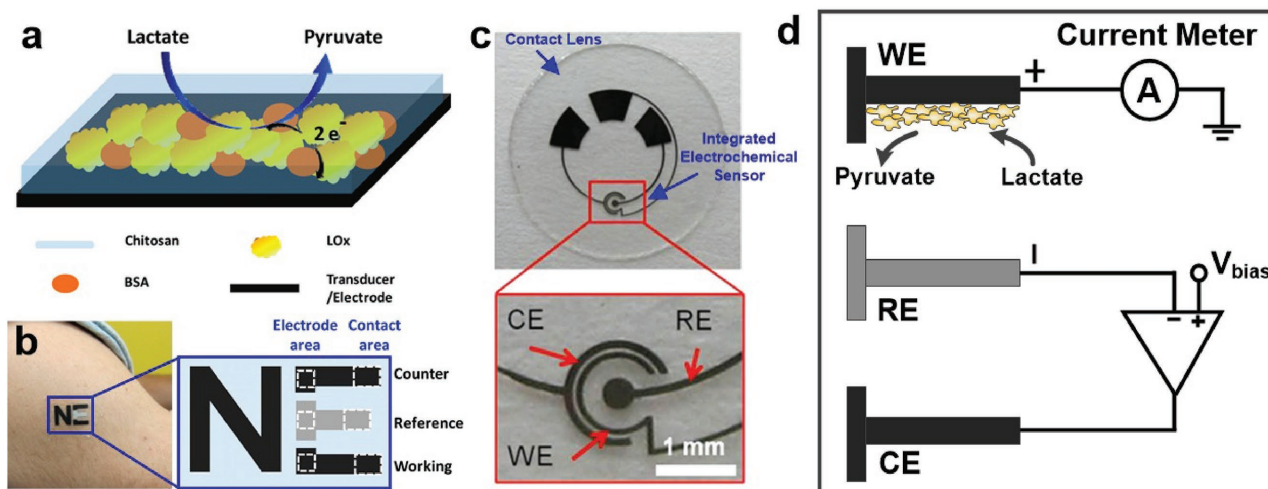


Figure 2. a) Simplified schematic of a working electrode for an electrochemical body fluid sensor and its application as planar cell for b) sweat sensors on a transferable tattoo^[15] and c) a tear sensor on a contact lens.^[69] d) Exemplary operation principle and sensing mechanism of electrochemical sensors. a,b) Reproduced with permission.^[15] Copyright 2013, American Chemical Society. c) Reproduced with permission.^[69] Copyright 2012, Elsevier.

While electrochemistry methods have since long been applied to the characterization of liquid mixtures, and electrochemical biosensors are well established analytical instrumentations, their application to continuous wearable sensors is relatively new. The translation of this approach has been previously challenged by the fabrication of robust electrochemical cells and circuitry that can be placed in continuous contact with the target body fluid. The development of flexible electronic micro-fabrication approaches has enabled the engineering of skin-like planar electrochemical cells that have been proven to work with the small amount of liquids available on the human iris and skin (Figure 2b,c). Typical layouts consist of a WE, CE, and RE electrodes deposited on flexible insulating and biocompatible substrates such as 2-methacryloyloxyethyl phosphorylcholine (MPC) polymer,^[11,28] polydimethylsiloxane (PDMS),^[11,28] and polyethylene terephthalate (PET).^[69] A major challenge is how to supply the required voltage for the required redox reactions. This is usually in the range of 0.4V^[11,28,69] and requires appropriate power sources and wiring. Furthermore, the readout of the generated current is also not trivial for measurements within the iris or mouth. As we will discuss in the following subsections, highly innovative and promising concepts have been proposed to address these challenges for different sensing environments.

3.1. Tear Sensors

Tear sensors are commonly integrated on the inner side of a flexible contact lens (Figure 2c and 3). The location of the electrodes and associated circuitry is on the perimeter of the iris and sufficiently distant from the pupil to avoid covering the field of vision. Typical transparent substrates are flat MPC, PDMS, and PET, which enable the deposition of electrodes and circuitry by sputtering,^[11] and CVD/PVD deposition^[70] or e-beam,^[69] followed by lithography and wet-etching approaches.^[71] Common

electrode materials include Ti/Pd/Pt,^[69,70,72] Pt/Ag/AgCl,^[11] and Au/Ag/AgCl^[28] with a rectangular or curved layout. A suitable anatomical shape is imparted to the originally flat substrates by moulding with heat and pressure.^[69,70,72] Monitoring of glucose and lactate concentrations has been a main focus of tear sensor studies (Table 1).^[11,28,69,70,72]

Recent studies have shown a direct correlation between tear and blood glucose concentration.^[11,73] Integration of glucose sensors into contact lenses has been achieved by several research groups,^[11,27a,70] who have been able to fabricate high-performance electrochemical sensors integrated in contact lenses for direct glucose monitoring in the iris (Figure 3). The electrochemical sensor usually consists of a working electrode functionalized with the glucose oxidase (GOD) enzyme, which results in the production of hydrogen peroxide and generation of a catalytic current between the working and counter electrodes. This approach results in miniaturized sensors that are highly selective to glucose and capable of easily detecting the required concentrations (ca. 1 μM) in tears. One persistent problem for these types of devices is the implementation of a suitable power source and readout system (Figure 3a).^[28] Integration of inductive links and radio frequency (RF) circuits has been successful in decreasing the required wiring and device size (Figure 3d).^[13a,72] In addition to the miniaturized RF sensor system, this approach requires a reader antenna coil system of sufficient size and power being in relatively close proximity (5–10 cm) to the device. As an alternative, integration of biofuel cells (BFC) into these bionic contact lens has been proposed.^[28] Enzyme catalysts were employed to convert the chemical energy from available biofuel (glucose) and biooxidant (oxygen) into electrical energy.^[28,74] However, for application as a power source for glucose-sensing, utilization of glucose from the same tear fluid may interfere with the accuracy of the measurements.

Falk et al.^[28] demonstrated a tetrathiafulvalene-tetracyanoquinodimethane/bilirubin-oxidase-based miniature BFC that

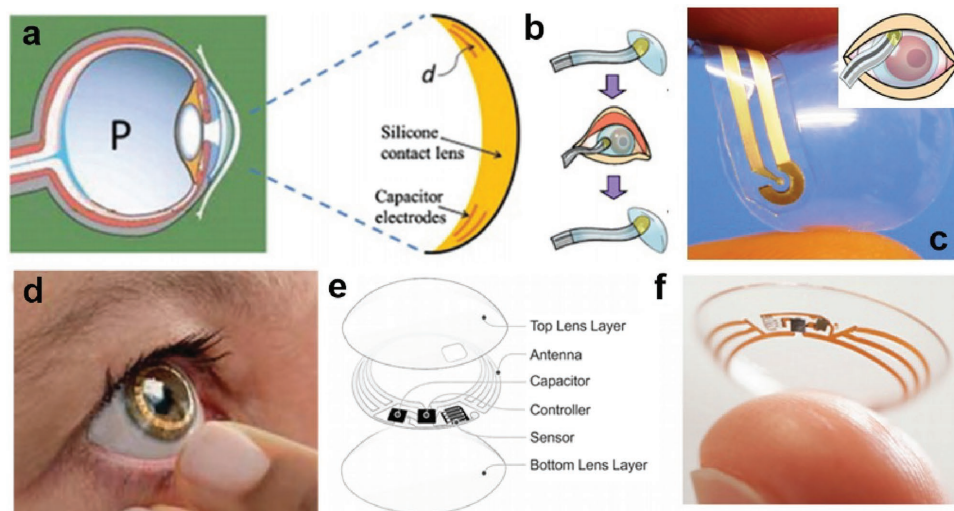


Figure 3. Schematic description of a–c) the placement of a contact lens with integrated sensor in the human iris. a–c) Reproduced with permission.^[11,68b] Copyright 2011, 2013, Elsevier. d–f) Demonstration and schematic of a more miniaturized wireless layout for glucose monitoring from tear analysis. d) Reproduced with permission.^[13a] Copyright 2013, Sensimed AG. e–f) Reproduced with permission.^[13b] Copyright 2014, Google X.

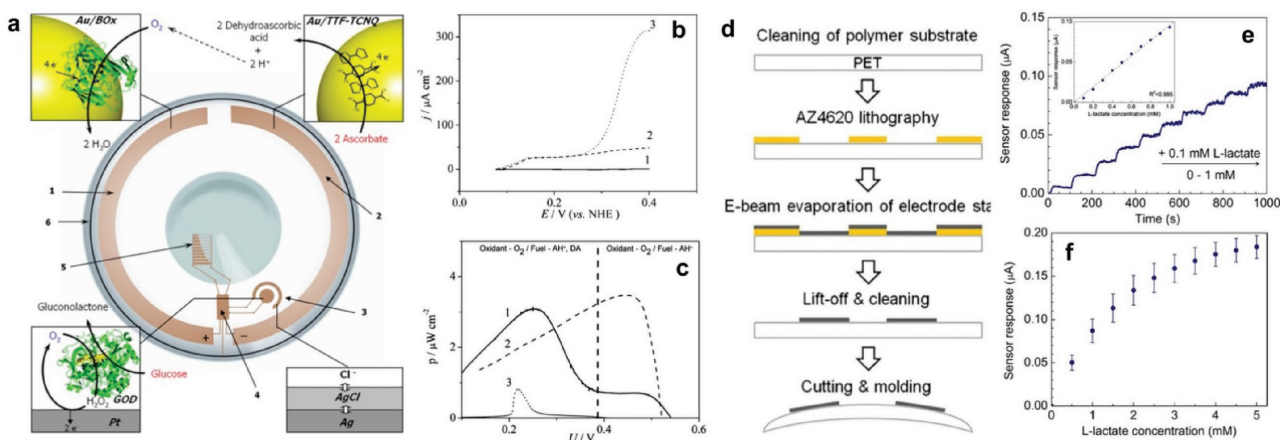


Figure 4. a) Schematic layout and b,c) characterization of an electrochemical sensor with an integrated biofuel cell (BFC) on a contact lens for tear glucose analysis. a–c) Reproduced with permission.^[28] Copyright 2013, American Chemical Society. b) Ex situ characterization of the electrochemical sensor response by supply of (1) 5 mM glucose (continuous line), (2) 5 mM glucose and 0.2 mM ascorbate (broken line) and (3) 5 mM glucose, 0.2 mM ascorbate, and 0.2 mM dopamine solutions (dotted line). c) BFC power density with (1) human basal tears (continuous line), (2) phosphate buffer saline (PBS) with 0.5 mM ascorbate (broken line), and (3) pure PBS (dotted line). d) Fabrication and e,f) characterization of a planar electrochemical cell on contact lens for L-lactate monitoring. e) Dynamic electrochemical response to increasing L-lactate concentrations and f) corresponding calibration curve from 0.5 to 5 mM. d–f) Reproduced with permission.^[69] Copyright 2012, Elsevier.

can generate ca. $3.1 \mu\text{W cm}^{-2}$ of power from the ascorbate and oxygen available in basal tears without influencing the glucose concentration (Figure 4a,b). Measurements were performed ex situ with a macrocell of 30 mL by chronopotentiometry using a three-electrode rotating disk with a Ag-AgCl₃ and a platinum wire mesh as reference and counter electrodes, respectively. While the device showed no sensor response to pure glucose solutions (Figure 4b, continuous line), a strong electrochemical sensor response was achieved with the addition of ascorbate (broken line) and ascorbate-dopamine fuels (dotted line). An open-circuit voltage of 0.54 V and a maximal power density of $3.1 \mu\text{W cm}^{-2}$ at 0.25 V were achieved with human basal tears (Figure 4c).^[28] This device was able to maintain a stable current density output of $0.55 \mu\text{A cm}^{-2}$ at 0.4 V over 6 h of continuous operation.

Thomas et al.^[69] reported an amperometric, mono-enzymatic L-lactate sensor on polymer contact lens for minimally invasive sampling of tear fluid (Figure 2c and 4d–f). The layout consists of an amperometric sensor based on a Pt working and reference electrode, and an auxiliary Pt counter electrode as a current drain (Figure 2c).^[69] This three-electrode configuration allows for a stable reference voltage between WE and RE. Flavoenzyme LO_x was utilized as a selective sensing element for L-lactate. The electrodes were deposited on 100- μm -thick PET substrates.^[69] All measurements were carried out ex situ at room temperature in phosphate-buffered saline (PBS) solution with a pH of ca. 7.4, which is used to mimic the physiological conditions on the surface of the eye.^[75] Appropriate amounts of the L-lactate enzyme were added to the PBS and the current response was recorded for 100 s following each addition (Figure 4e,f).^[69] A voltage of 0.4 V was used for all measurements, as it was found to show optimal signal characteristics. This work demonstrates sensing down to 0.1 mM concentrations of L-lactate (Figure 4e) by a flexible and relatively simple three-electrode configuration.^[69] Future work is required to extend this approach for in situ measurements where supply

of stable voltages and data readout from the pupil remain challenging tasks.

3.2. Saliva Sensors

A major advantage of saliva analysis is the large amount of fluid available and the significantly larger space usable for the localization of the devices. Furthermore, in contrast to tear analysis, the mouth is also a less delicate environment for the incorporation of implants and can benefit from the extensive research in biocompatible materials pursued for dentistry. Several studies have presented salivary sensors based on screen-printing techniques that offer scalable low-cost fabrication.^[55b,76] However, the realization of wearable biosensors for real-time monitoring of chemical markers has been limited by the small number of demonstrated measurable analytes (Table 1) and the lack of integrated wireless data transmission.^[21a,77]

Mannoor et al.^[14] recently reported a graphene-based wireless resistometric sensor for continuous monitoring of bacteria on a silk dental tattoo platform (Figure 5a–d). Graphene is particularly interesting for flexible electronic applications due to its remarkable electrical conductivity and mechanical properties having an intrinsic strength of 42 N m^{-1} and Young's modulus of $\approx 1 \text{ TPa}$.^[78] Furthermore, graphene's high interfacial adhesion to many substrates^[79] enables its applications to many sensor layouts and materials.^[80] In this study, self-assembly of antimicrobial peptide (AMP), consisting of dodecapeptide graphene-binding peptide, a triglycine linker and the AMP odorant-HP, onto graphene was utilized to achieve bioselective detection of bacteria at single-cell levels.^[14] Upon recognition and binding of specific bacterial targets by the immobilized peptides, the electrical conductivity of the graphene film varies (Figure 5e). This is wirelessly monitored using an inductively coupled radio frequency (RF) reader device. To investigate the performance of the sensor when directly integrated with

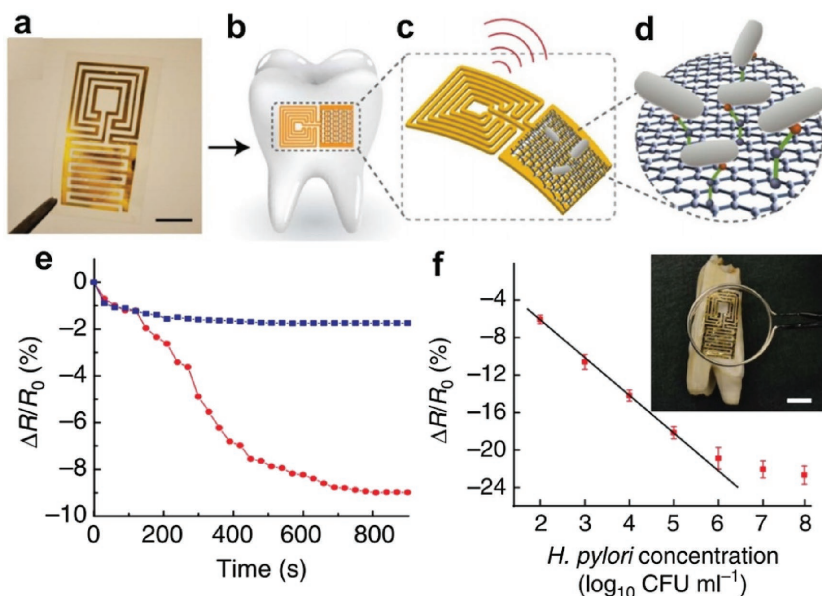


Figure 5. a–d) Demonstration of a graphene-based wireless resistometric sensor for continuous monitoring of bacteria on a silk dental tattoo platform. The scale bar in panel (a) is 0.7 cm. This device shows a clear response upon e) exposure to 1 μL samples of human saliva containing ca. 100 *H. pylori* cells (blue squares), and nearly no response to pure saliva without bacterial cells (red circles). f) A logarithmic relationship was observed between the bacteria concentration and the change in resistance up indicating a lower detection limit of ca. 100 cells. Inset shows the incorporation on a bovine tooth with a scale bar of 1 cm. a–f) Reproduced with permission.^[14] Copyright 2012, Nature Publishing Group.

biological tissue, the sensor was transferred onto the surface of a bovine tooth (Figure 5f, inset). Future work is required to demonstrate the application of this concept for the measurement of salivary metabolites such as glucose^[38,41] and caffeine^[34] as well as to further decrease the size of the antenna to a size suitable for integration on human teeth.

Kim et al.^[55c] developed an electrochemical sensor on a mouthguard integrated with a bluetooth low energy communication system-on-chip for continuous real-time amperometric monitoring of uric acid (Figure 6a). A three-electrode layout with a uricase enzyme-modified surface was screen-printed on the mouthguard (Figure 6a,b). To assess the validity of this

presence of batteries within the mouth cavity may bring additional risks and challenges for long-term utilization.

3.3. Sweat Sensors

Sweat analysis offers some advantages over tear and saliva. The skin is the largest organ of the human body and provides a very large surface for the placement of and interaction with the sensor surface. It is, commonly, less delicate than the human pupil and mouth cavity. Commercially available wearable electronics, in relatively close contact with skin, already exist and

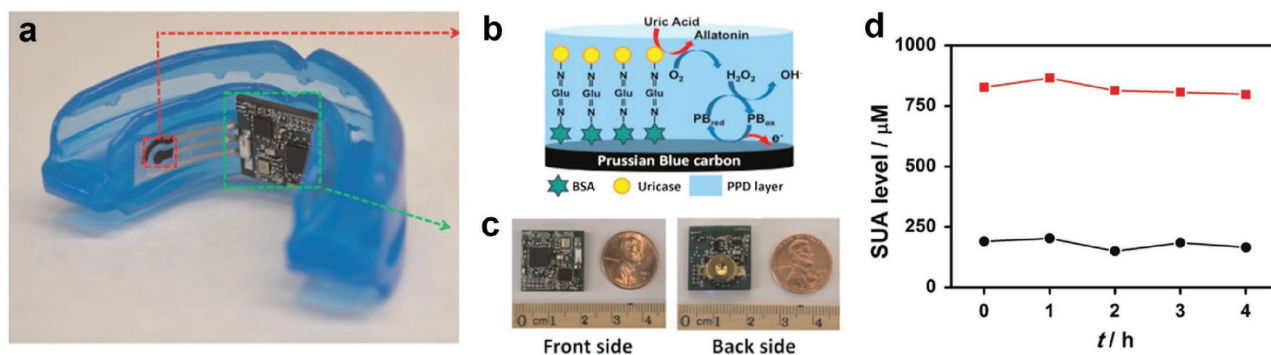


Figure 6. Demonstration of a) an electrochemical uric acid sensor integrated on a mouthguard with a bluetooth low-energy communication system-on-chip. b) A selective working electrode was achieved with uricase enzyme-modified surface. c) The device fits on a square with a side of ca. 2 cm. d) Monitoring of the uric acid concentration of a healthy control (black circles) and a hyperuricemia patient (red squares) shows its potential application for non-invasive diagnostics of hyperuricemia. All panels reproduced with permission.^[55c] Copyright 2015, Elsevier.

can provide power and readout opportunities for the sensors. However, a major challenge is that secretion of sweat can vary largely during the day and as a function of the activity level. In rest conditions, the amount of sweat available for analysis can be significantly lower than tear fluid in the pupil, and orders of magnitude smaller than the available saliva in the mouth. The skin is also more subject to potential contaminants that bring additional unknown variables in the system. Furthermore, utilization of a large skin surface to enhance the available surface for sweat collection requires not only flexible but also stretchable ultra-light sensors which do not interfere with mobility requirements and sensory feelings.^[21a,b,26b] The biocompatibility of the interface between the skin and sensor needs to be carefully tested to avoid allergic reactions and potential inflammations.^[81]

In 2010, Schazmann et al.^[21b] presented the monitoring of sodium content in human sweat by a sensor belt (Figure 7a) consisting of sweat-wicking materials and ion selective electrodes (ISE). The relatively bulky assembly was pressed against the subject's back by a belt, and enabled measurement down to 20 [Na]/mM. Liu et al.^[26b] introduced a more compact wearable conductivity sensor for wireless real-time monitoring of sweat's electrolyte content (Figure 7b,c). Sweat was continuously sampled through a PDMS collector connected to a 22 gauge Teflon tube. A hole of 1.2 mm diameter, placed at the bottom of the PDMS collector, was in direct contact with the skin, covering ca. 1.5 sweat glands on a dorsal forearm. The pressure difference between the skin and sweat glands and the capillary pressure push the sweat up the tube. As sweat passes through the tube its conductivity is measured between two calibrated wires allowing for real-time analysis. The data was transferred to a printed circuit board (PCB) with a HC-06 bluetooth transceiver, which wirelessly transmitted to a Windows phone. The

whole device was packaged into a wristwatch (Figure 7b). The accuracy of these measurements was validated with a Horiba LaquaTwin conductivity sensor.

Recent achievements in stretchable electronics and biocompatible tattoos are revolutionizing the design of wearable devices for sweat analysis.^[21a,82] Many successful implementations are based on papilio transferable enzymatic tattoos with silver/silver chloride and carbon ink electrodes and circuitry that show excellent biocompatibility.^[15,21a,82] Jia et al.^[15] developed an electrochemical lactate sensor on a tattoo (Figure 7d) for real-time monitoring of human perspiration. The device consists of three electrodes made from a base of chopped carbon fibers dispersed within conductive carbon ink on the working and counter electrodes, and silver/silver chloride inks on the reference electrode (Figure 2b). The carbon fibers are used to increase the tensile strength of the electrodes to conform to the body. A selective lactate working electrode was achieved by coating its surface with a mixture of LOx enzymes tethered to tetrathiafulvalene (TTF) and multi-walled carbon nanotubes (CNT). A chitosan top-coating was used to enhance biocompatibility and prevent the catalytic backbone flowing onto the epidermis (Figure 2a). Data collection was achieved from the skin-adherent patch via wires connected to a computer. It was observed that, in contrast to the bare controls (Figure 7e, line b), the LOx-functionalized devices (Figure 7e, line a) were capable of detecting lactate in the perspiration. Detection down to 4 mM of lactate was achieved using a potential step to +0.05 V vs Ag/AgCl, which led to a catalytic current of ca. 4 μ A.

Kim et al.^[82] presented a wearable tattoo-based iontophoretic-electrochemical sensing system for monitoring of sweat alcohol content (Figure 8a,b). Sweat alcohol content is strongly correlated with blood alcohol concentration (BAC) and is an

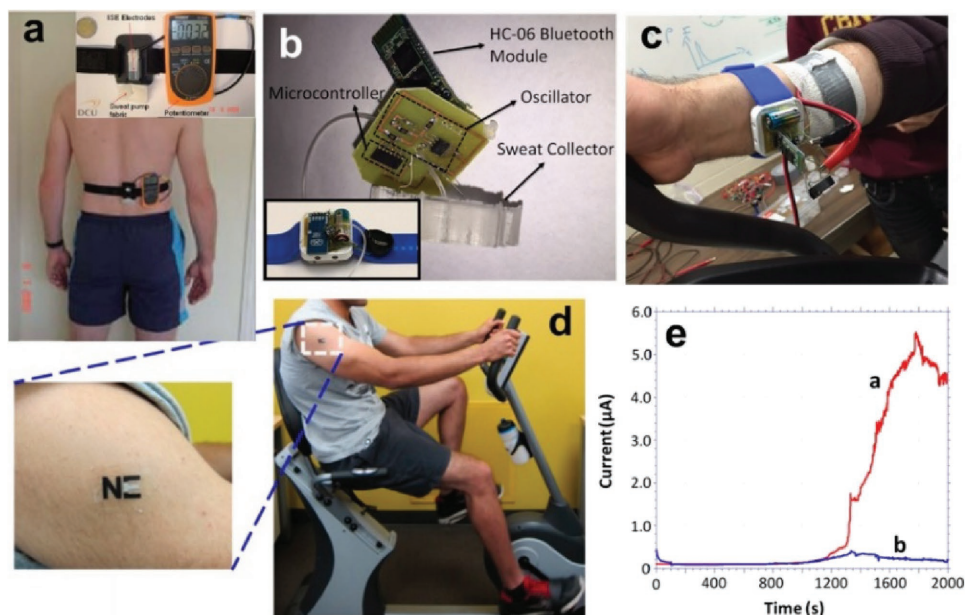


Figure 7. Sweat sensor layout for a) sodium content analysis with a sensor belt (Reproduced with permission.^[21b] Copyright 2010, Royal Society of Chemistry), b,c) electrolyte content analysis with a conductivity sensor integrated in a bluetooth-capable wristwatch (Reproduced with permission.^[26b] Copyright 2016, Elsevier), and d–e) lactate monitoring with an electrochemical planar cell on a transferable tattoo. This LOx functionalized sensor enables e) real-time measurement of lactate (line a) while the non-functionalized control (line b) shows no clear response. d,e) Reproduced with permission.^[15] Copyright 2013, American Chemical Society.

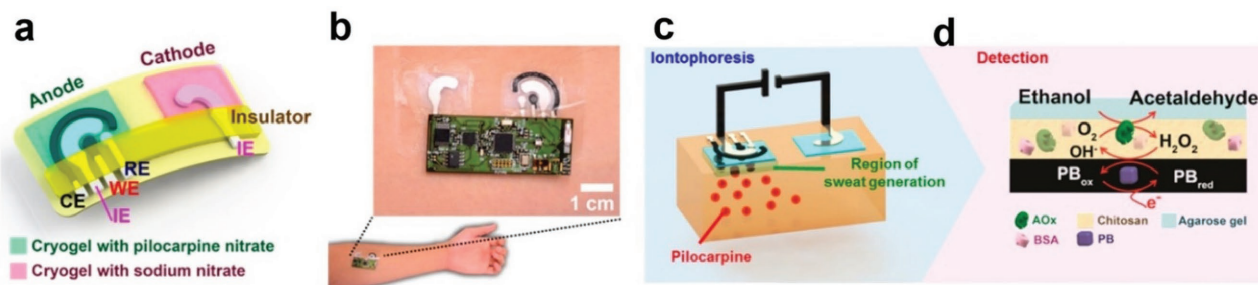


Figure 8. a,b) Schematic of a wearable tattoo-based iontophoretic-electrochemical sensing system for monitoring sweat alcohol content (SAC). Release of pilocarpine to the skin is utilized to induce sweat.^[82] c) The device is integrated on a printed circuit board of a few cm with bluetooth capability for wireless data transmission. d) Selective measurement of SAC is achieved with AOx receptor and Prussian Blue transducer.^[82] All panels reproduced with permission.^[82] Copyright 2016, American Chemical Society.

alternative non-invasive source for alcohol monitoring.^[82] A major achievement of this study is the development of a well-controlled sweat sampling system. Sweating can be induced by pilocarpine iontophoresis, removing some of the challenges for its sampling. Pilocarpine can be delivered across the skin by applying a constant current between an anode and a cathode (Figure 8c). Sweat will then flow from the anode to the cathode along the skin. In this study, the application of a 0.6 mA current for five minutes was found to provide sufficient sweat generation while remaining imperceptible to humans. The electrodes consisted of a Ag/AgCl reference electrode and Prussian Blue (PB)-conductive carbon working and counter electrodes. The surface of the working electrode was coated with alcohol-oxidase (AOx) enzyme mixed with a bovine serum albumin (BSA) stabilizer and a chitosan solution with PB as the transducers (Figure 8d). The functionalized working electrode was then covered with an agarose gel to buffer the effect of pilocarpine on the PB electrode. The device had a size of 3×4 cm (Figure 8b). Reaction of O_2 and ethanol on the AOx results in acetaldehyde and H_2O_2 , and oxidation of the PB, which results in a current flowing across the electrodes (Figure 8d). The entire measurement was automated by placing these electrodes in the region where the pilocarpine iontophoresis had induced sweating (Figure 8d). The electrodes were connected to a PCB containing a bluetooth low-energy system-on-chip that allowed for data transmission to a laptop. The PCB was powered by two watch batteries of 33 mA h and 1.55 V each. The measured concentration of sweat alcohol was compared to the BAC level measured with a commercial Alcovisor Mars Breathalyzer, showing a correlation of $r = 0.912$.

4. Volatile Biomarker Analysis and Miniaturized Gas Sensing Systems

Non-invasive medical diagnostics by detection of volatile biomarkers produced by our metabolism is an ancient approach that has been known since the dawn of medical sciences. Hippocrates mentions breath analysis in his treatises on breath aroma and diseases. As early as the mid-1800s, the presence of acetone in the breath was found to be related to diabetes.^[83] Volatile organic compound (VOC) analysis from human breath and skin perspiration is amongst the least invasive and

instinctive methods of medical diagnostics. It also offers unique advantages for the continuous measurement of important biomarkers, as it does not need to be placed in direct contact with any part of the body or immersed in a body fluid. Despite this early start and potential, volatile biomarker analysis has not played a major role in clinical diagnostics. This is mainly due to the challenges associated with the precise measurement of ultra-low concentrations of gas molecules in very complex gas mixtures such as the human breath. This has delayed the establishment of a robust set of VOCs and levels associated with specific diseases and metabolic states. Exemplary exceptions are the measurement of ammonia for diagnosis of helicobacter pylori infections of the stomach,^[84] and more recently exhaled NO (eNO) concentrations for diagnosis of asthma.^[85]

The use of volatile biomarker analysis is becoming increasingly attractive due to the development of powerful analytical tools for lab-scale analysis of ultra-low concentrations of VOCs from body fluids, including breath, skin, urine, and blood. Volatolomic approaches are now emerging as a powerful alternative for the continuous monitoring of key metabolic processes in our bodies. In fact, VOCs released from their origin and/or fat compartment storage into the circulatory system^[86] can be directly detected from blood^[87] and the headspace of cells.^[88] VOCs can also be externally emitted by several secretion pathways including exhaled breath,^[87a,89] skin/sweat,^[90] feces,^[91] urine,^[92] saliva,^[55b,c,76,93] and others, such as breast milk.^[94] Secretion of ca. 2,600 VOCs from healthy subjects have previously been characterized,^[86b,95] mostly from a single secretion pathway.^[86b,95] The nature, origin, emission, and related biochemical pathways of endogenous and exogenous VOC families, primary and secondary alcohols, aldehydes and branched aldehydes, ketones, esters, nitriles, and aromatic compounds in volatolomics have recently been reviewed thoroughly.^[86,95a,96] Table 2 presents a short summary of some VOCs and associated diseases detected by common pathways. A key challenge facing volatolomic approaches for personalized and preventive medicine is the development of miniaturized low-power chemical sensors capable of selective sensing of a few particles per billion concentrations of VOCs in the presence of high concentrations of water vapor and other gases.^[97] Meaningful VOCs analysis requires stable and reproducible responses and elimination of additional factors such as gender, age, and smoking status.^[98]

Table 2. List of some common volatile biomarkers and sensor technologies for the most established pathways.

Pathway	Biomarker	Purpose	Levels	Sensor technology	Ref.
Breath	Acetone	Hyperglycemia	30 ppb	Si-doped WO ₃ nanoparticle films	[97b]
	Ammonia	Liver failure	50 ppb	Chemoresistive Nano-MO _x ^{a)}	[104]
	Ammonia	Liver failure	10 ppb	p-n oxide semiconductor heterostructure	[105]
	2-Butanone	Helicobacter pylori	500 ppb	Chemoresistive graphene-ZnO	[106]
	Ethanol/toluene	Alcohol/cigarette consumption	0.1 ng	Hadamard transform GC-MS ^{b)}	[107]
	H ₂ S	Asthma	534 ppt	Chemoresistive	[108]
	NO	Lung injury	206 ppt		
	Menthone	Amount of cigarettes smoked	≈ ppt	Atmospheric pressure chemical ionization	[109]
	C ₈ H ₈ , C ₉ H ₁₈ O 2-EH, C ₇ H ₁₄ O, C ₁₀ H ₂₀ O, C ₁₆ H ₃₄	Ovarian cancer	400 ppb	Chemoresistive flexible nanoparticle-based sensor array	[110]
	Trimethylamine	Chronic kidney disease	1.76 ppb	GC-MS ^{b)}	[111]
Skin perspiration	Acetone	Diabetes	10 ppb	Chemoresistive MO _x with zeolite concentrators	[18]
	CO ₂	Respiration monitoring	60 ppb	Optical coherence tomography	[112]
	DMMP	Atmospheric nerve gas	5 ppm	PPy coated graphene field effect transistor sensor	[113]
	Ethene	UV radiation	1.4 pmol kg ⁻¹	Photoacoustics	[114]
	Glucose	Diabetes	50 mg dL ⁻¹	Mid-infrared spectroscopy	[115]
	Water vapor and oxygen	Respiratory distress in infants	NR ^{c)}	Laser spectroscopy	[116]
	C ₃ H ₆ O ₃ C ₃ H ₄ O ₃	Gastric cancer	0.1 × 10 ⁻⁶ M	Potentiometric with Lactate Oxidase-functionalized ZnO	[117]
Digestive System	Malonic acid and L-serine	Esophageal cancer	50 × 10 ⁻⁶ M	GC-MS ^{b)}	[118]
	Lactic, aminovaleric, and glyoxylic acids	Various cancers	1 μg mL ⁻¹	Ratiometric fluorescence	[119]
					[120]
	L-alanine glucuronic lactone L-glutamine	Colorectal cancer	0.01 × 10 ⁻⁶ M	Amperometric biosensor based on nanoporous nickel/ boron-doped diamond film	[121]

^{a)}MO_x: metal oxide semiconductors; ^{b)}GC-MS: gas chromatography and mass spectrometry; ^{c)}Not reported.

Arrays of nanomaterial-based sensors, often termed as nanoarrays,^[99] have great potential to meet these clinical challenges and become powerful diagnostic tools owing to the inherently non-invasive nature of volatolomics. The large surface-to-volume ratio of the nanomaterials provides high sensitivity and fast response and recovery times. The broad range of well-investigated nanomaterials can help to increase the selectivity and sensitivity to the target VOC.^[97a] Their small size also allows on-chip integration of large arrays.^[8a] Development of novel solid-state sensors for selective detection of ultra-low concentrations of specific gas molecules is becoming increasingly more feasible due to the recent progress in nanofabrication approaches, which are capable of providing atomic-level control of the surface composition of high-surface-area detectors.^[100] Common VOC sensing mechanisms for wearable and miniaturized sensors include chemo-resistive semiconductors,^[97a,101] surface acoustic wave resonators,^[102] and capacitive polymers.^[62,68a] The sensing mechanism of semiconductor chemo-resistive sensors has been recently summarized in.^[97a] In short, the conductivity of a nanostructured sensor film changes significantly as a function of the concentration of reducing and oxidizing gases and their reactivity with the semiconductor surface. This technology enables the particle-per-billion detection of important VOCs such as acetone^[97a] and ethanol^[103] by a simple and highly miniaturizable resistance measurement.

Surface acoustic wave (SAW) resonators are based on the modulation of acoustic waves traveling between reference points in a medium.^[102] The presence of analytes in the medium influences factors of the wave such as its speed and amplitude. The substrate used in a SAW resonator has piezoelectric properties that allow transversal waves to propagate across the surface.^[122] When a receptor is adhered to the surface, whether through adsorption or some other kind of reaction, the reception of the wave will be modified due to changes in the wave characteristics.^[123] SAW resonators have been used as an immunoassay format,^[122] for the detection of VOCs such as ethanol, acetone, and propanol,^[124] and as part of gas chromatography for the early screening of lung cancer.^[125]

Capacitive polymer sensors are based on dielectric layers with imprinted polymers on the surfaces. A surface insulated with a polymer coating will change in thickness or dielectric constant when certain analytes are in the environment.^[68a] This change can be detected by changes in the capacitance or impedance of the capacitor itself, and the degree of this change is proportional to the concentration of the analyte. Ultrathin polymer layers are used in capacitive polymer sensors, and they are typically fabricated by electropolymerization.^[126] Capacitive sensors have been used for the detection of lipolytic enzymes,^[11] surfactants,^[14] and as immunosensors.^[62] In the following subsections, we will present some successful designs that have

demonstrated particular merits for the development of miniaturized and wearable VOCs measurement.

4.1. Breath Analysis and Miniaturized Gas Sensor Systems

A major advantage of breath analysis is that the concentration of VOCs is usually some orders of magnitude higher than that perspired through the skin (Table 2). A standing challenge is how to sample precise and reproducible parts of the breath during the correct exhalation phase without increasing the size and complexity of the device. In laboratory experiments, this is usually achieved by carefully designed systems including valves, heated masks, and lines that avoid condensation of VOCs and can select the breath component to be analyzed. Achieving the same effect with portable hand-held or wearable devices is not trivial. A major disadvantage of breath and other VOC analysis compared to body fluid analysis is that the latter can more easily achieve selectivity due to the functionalization of the working electrode surface with readily available biological enzymes. Current approaches for overcoming these challenges are often based on pattern analysis from an array of diverse gas sensor components. Despite these challenges, breath analysis is showing some promising results for the very early-stage and self-diagnostics of numerous diseases such as several types of lung^[127] and breast^[88a] cancers, and chronic inflammatory and metabolic diseases such as asthma^[85] and diabetes.^[10]

Barash et al.^[88a] recently reported the mapping of molecular subtypes in breast cancer (BC) tumors by GC-MS and nanostructured sensor arrays analysis of breath samples collected from 276 volunteers, including benign conditions, ductal carcinoma in situ (DCIS), malignant lesions, and healthy controls (Figure 9a–d). GC-MS analysis revealed up to 23 compounds that were significantly different in the breath of breast cancer patients having distinct molecular subtypes (Figure 9c). Application of discriminant function analysis (DFA) to the response of the nanostructured sensor arrays analysis (Figure 9d) enabled differentiation with 83% accuracy between cancer and non-cancer cases, and 82–87% accuracy between different molecular subtypes. Similar nanostructured sensor array approaches^[128] have been utilized recently (Figure 9e,f) for detection of preeclampsia, a hypertensive disorder of pregnancy, which is a leading cause of maternal and perinatal morbidity and mortality. Molecularly modified gold nanoparticle sensor arrays were “trained” for characterizing the breath print of preeclampsia, which have higher concentrations of some specific VOCs such as octanal and C₁₃H₂₈. The nanoparticle sensor arrays were able to distinguish preeclampsia from healthy pregnant women with an accuracy of 84%.

A major challenge in developing sensor array systems for breath analysis is the development of sufficiently selective and distinct sensing materials. In 2010, Righettoni et al.^[100b,129] reported the synthesis of a highly selective nanostructured material for acetone sensing, a major breath marker for diabetes (Table 2). Films of Si-doped WO₃ nanoparticles^[100b,129] were deposited by flame synthesis on a simple interdigitated electrode layout (Figure 10a) and capable of chemoresistive measurement of down to 20 ppb of acetone at 90% relative humidity. The potential of this compact sensor layout for

online measurement of acetone was thereafter confirmed in real human breath by comparison with proton transfer reaction (PTR-MS), showing excellent accuracy (Figure 10b). A fully hand-held version of this technology for direct measurement of breath acetone has been presented recently (Figure 10c).^[10] Further miniaturization of this type of chemoresistive sensor is possible, enabling devices as small as few millimeters in size.^[130] Several research groups are developing carefully engineered sensing nanostructures for selective and room-temperature^[131] detection of important VOCs.^[132,133] Light activation of the sensing nanomaterial^[134] may further help in decreasing the operation temperature and increase the selectivity. Development of flexible and stretchable sensing materials has recently shown the potential to offer additional opportunities to increase the selectivity of these nanostructured sensors. Kahn et al.^[110] presented a flexible nanoparticle-based sensor array (Figure 10d) for diagnosis of ovarian carcinoma from exhaled breath. Strain-related response of functionalized gold nanoparticle sensors (Figure 10e) was utilized to successfully discriminate between the breath collected from ovarian cancer patients and control subjects with 82% accuracy from single sensors. Figures 10f,g show a schematic of the operation principles of a chemoresistive gas sensor. Usually, a constant voltage is applied between two interdigitated electrodes connected through a nanostructured semiconductor layer such as a film of SnO₂ and WO₃ nanoparticles. The latter is commonly kept at a constant temperature in the range of 200–400 °C, and engineered to promote the reduction or oxidation of the target analyte. These redox reactions change the concentration of surface charges on the nanostructured film changing the material conductivity, and increasing or decreasing the current flowing between the two electrodes. If the size of the nanostructures is comparable to the Debye's length of the semiconductor, the change of conductivity affects the whole material, and can result in several-orders-of-magnitude-strong current rise or decay already at analyte concentrations of few ppm.^[97a]

4.2. Skin Perspiration Analysis and Wearable Sensing Devices

Similar to sweat analysis, skin perspiration analysis is receiving increasing attention and research efforts due to its facility of placing relatively large devices on the surface of the body without causing significant discomfort. This facilitates the development of fully automated sensor systems for continuous monitoring of key biomarkers. Another advantage is that, in contrast to breath analysis, perspiration from the skin is relatively clean from exogenous gas molecules, and thus does not require, per se, careful selection of the exhalation phase to be analyzed. Compounds travel to the dermal layer through the interstitial fluid between blood vessels. There is a degree of leakage and osmosis from a blood capillary to the interstitial fluid, which enters the dermal layer.^[135] A major challenge is that the concentration of VOCs is significantly lower than in the breath (Table 2), requiring lower limit of detections in the low ppb–ppt level. Several approaches are being proposed to overcome this severe constraint, including chemical stimulation of the release of specific compounds^[82] and innovative concentrator approaches.^[18] This research area is also greatly

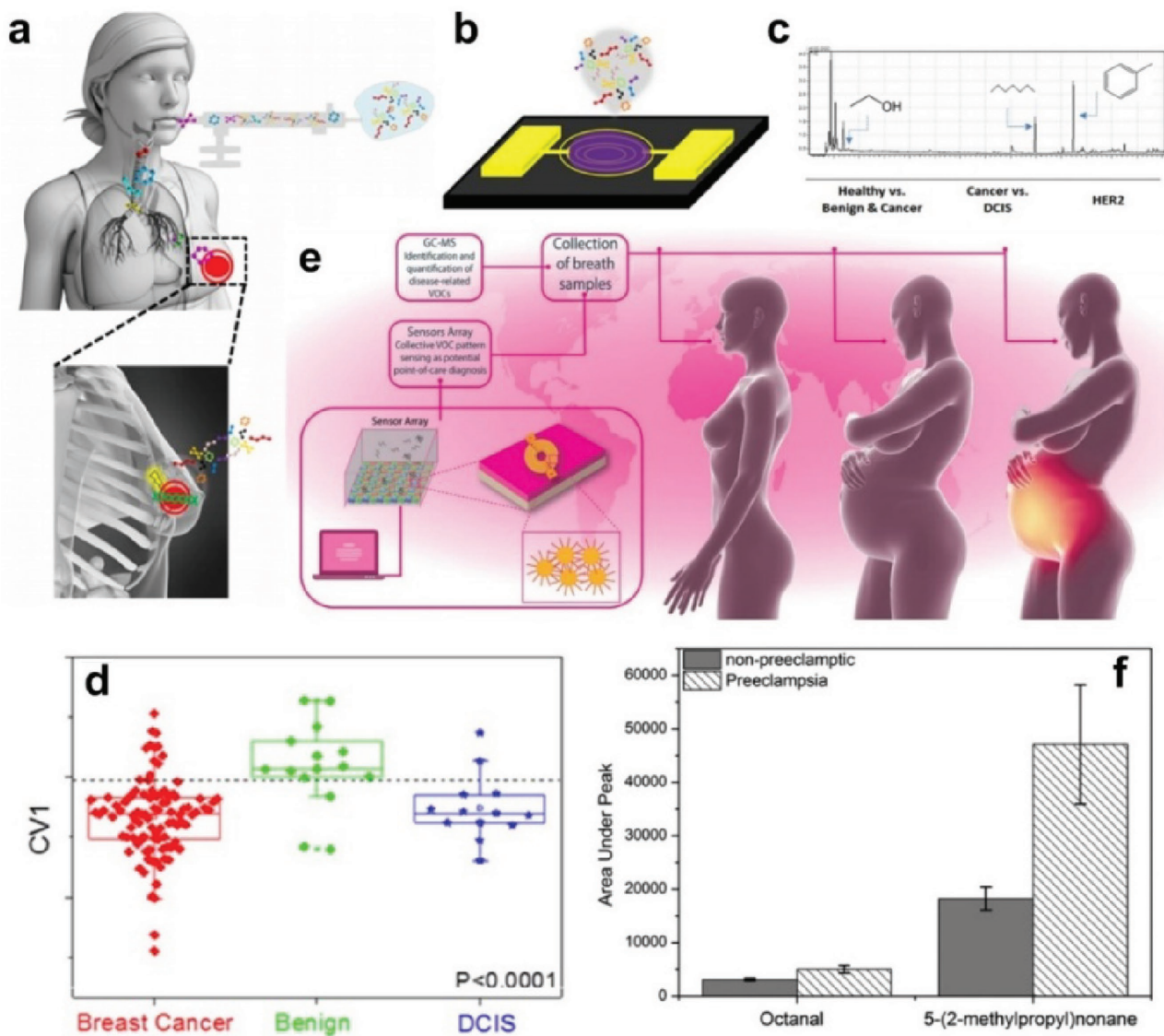


Figure 9. a) Schematic of breath sampling for b) nanostructured sensor array and c) GC-MS analysis of molecular subtypes in breast cancer. d) Differentiation amongst benign conditions, ductal carcinoma in situ (DCIS), and breast cancer was demonstrated with the nanostructured sensors array.^[88a] a–d) Reproduced with permission.^[88a] Copyright 2015, Oncotarget. e) Diagnostics of preeclampsia via breath analysis demonstrating f) a distinct set of VOCs for preeclampsia subjects.^[128] e, f) Reproduced with permission.^[128] Copyright 2016, Wiley Online Library.

benefitting from the development of flexible and transferable electronics that have been discussed in subsection 3.3 above.

Park et al.^[113] very recently reported a dimethyl methylphosphonate (DMMP) gas sensor on a highly stretchable and transparent patch, which can be placed on human skin and other surrounding objects (Figure 11a,b). DMMP is a stimulant of nerve gas, and its sensing by miniaturized sensor has immediate applications in workplace safety and defense. Hybrid nanostructures made of silver nanowires and graphene were used as electrodes and an RF antenna. A field-effect transistor sensor was obtained by drop-coating polypyrrole (PPy) onto graphene. This device was able to detect as little as 5 ppm of DMMP and sustained this ability to up to 20% strain. Good selectivity against acetone, methanol, water, and tetradecane was observed. While this device layout has not been imple-

mented for VOC monitoring, its compactness, wireless, and power-less capabilities makes it particularly interesting for skin perspiration analysis.

Yamada et al.^[18] proposed a zeolite-based concentrator for measurement of the acetone perspired through the skin with miniaturized chemoresistive gas sensors (Figure 11c–e). The latter are based also on highly responsive WO₃ nanostructures such as those reported previously for breath analysis.^[100b,129] The 390HUA zeolites were capable of adsorbing and desorbing approximately 100% and 90% of the injected acetone. The release of the acetone from the zeolite can be triggered either by heating or collapsing of the cavities through mechanical strain. Measurement of the skin perspiration for 10 min from 6 volunteers and comparison with GC-MS measurements demonstrated lower limits of detection down to 5 ppb (Figure 11e). Overall, this

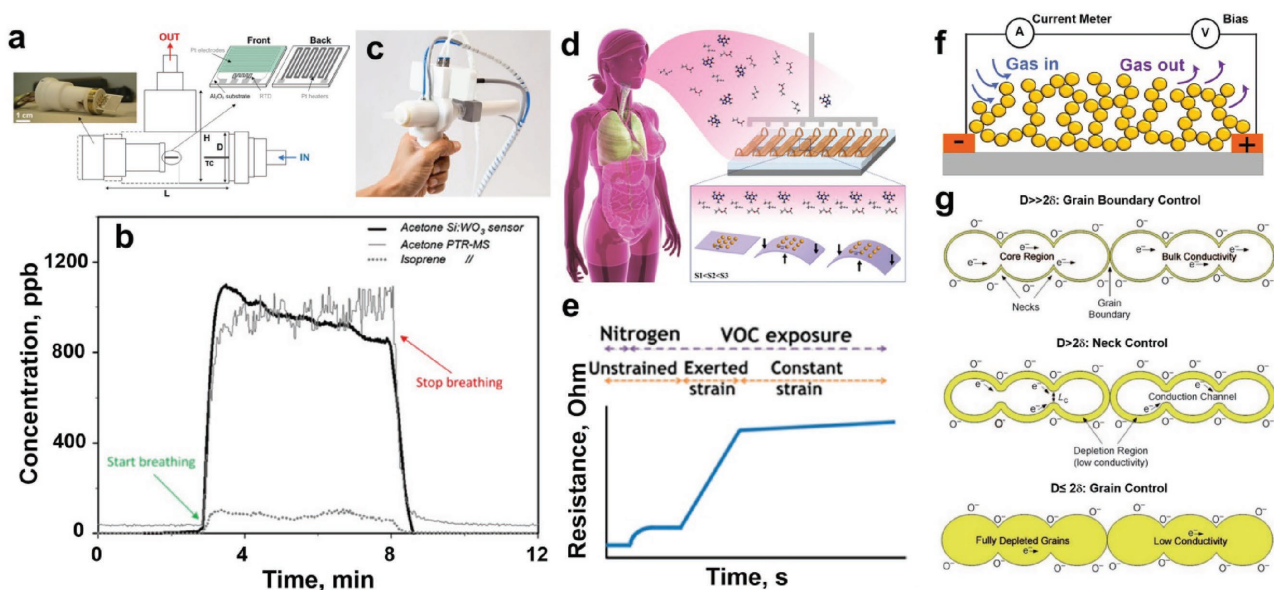


Figure 10. a) Schematic and demonstration of a compact chemoresistive device for breath acetone measurement for diabetes diagnostics showing b) excellent accuracy with PTR-MS measurements^[10] a,b) Reproduced with permission.^[10] Copyright 2012, Elsevier, and c) integration in an handheld device^[17] Reproduced with permission.^[17] Copyright 2015, Institute of Physics Publishing. (d) Schematic and e) characterization of a flexible gold nanoparticle sensor arrays for accurate strain-aided detection of ovarian carcinoma from breath analysis.^[110] d,e) Reproduced with permission.^[110] Copyright 2015, American Chemical Society. g) Exemplary operation principle and sensing mechanism^[97a] of chemoresistive sensors. Reproduced with permission.^[97a] Copyright 2010, Wiley Online Library.

approach has the potential to facilitate the development of skin transpiration gas analysis systems. Significant efforts are also being directed toward the development of low-power consumption detectors which are capable of selectively measuring small ppb concentrations of important VOCs. Multi-nanostructured

layers of CuO and SnO_2 nanoparticles have demonstrated chemoresistive detection of 20 ppb of ethanol,^[103] while transparent WO_3 nanocolumn morphologies have been utilized for the development of fully metal-oxide devices with ultra-low-power consumptions of 21.6 to 251 μW .^[101]

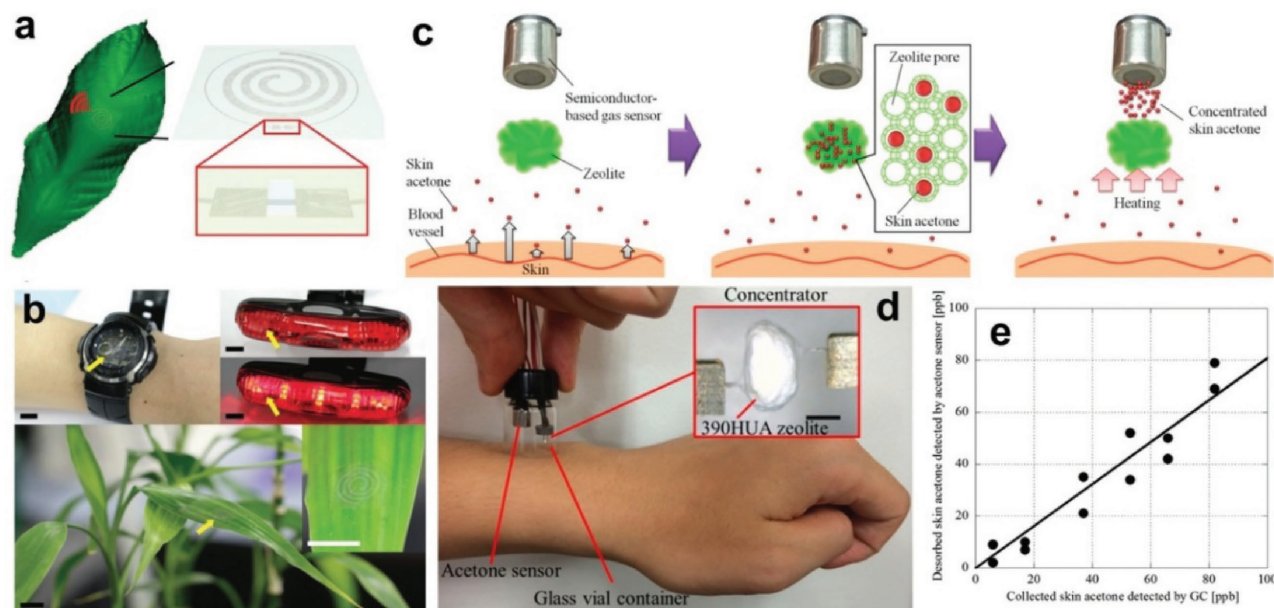


Figure 11. a,b) Schematic and demonstration of a flexible and transparent dimethyl methylphosphonate (DMMP) gas sensor based on PPy coated graphene field effect transistor sensors.^[113] a,b) Reproduced with permission.^[113] Copyright 2016, Royal Society of Chemistry. c) Schematic of zeolite collector for acetone monitoring through skin perspiration. d) Demonstration of an integrated skin perspiration sensor based on a 390HUA zeolite and a chemoresistive sensor and e) its validation against GC measurements.^[118] c–e) Reproduced with permission.^[118] Copyright 2015, American Chemical Society.

4.3. In Situ Digestive System Analysis and Swallowable Gas Sensors

In situ analysis of the digestive system is the least invasive procedure of a traditionally very invasive discipline. The huge amount of discomfort associated with procedures such as colonoscopies and endoscopies is evident from the reduced patient compliance to undergo a procedure, and the rates at which patients avoid heavily recommended repeat procedures. It has been estimated that as many as 40% of patients refuse to repeat a colonoscopy when advised to do so by a medical practitioner.^[136] In this context, a digestive system analyzer such as a smart gas^[12] and/or optical^[137] sensing system integrated in a swallowable pill can provide key information on the state of our digestive system with significantly less discomfort. This approach has also potential for simultaneous analysis and treatment procedures, where the pill may release highly concentrated and localized drugs in specific locations determined by the analysis of the surrounding area. In 2015, Kalantar et al. demonstrated a swallowable capsule capable of gas measurement in a pig's intestinal system (Figure 12). The capsule consists (Figure 12a–c) of an indigestible and impermeable shell with a gas-permeable membrane; a gas sensor for H₂, CH₄, or CO₂, which are commonly found in the gut; a microcontroller; a wireless transmitter; and a silver oxide battery. The gas-permeable membrane is made of polydimethylsiloxane with embedded nanoparticles, which are utilized to increase the permeability to the target gas molecules. The voltage output of the sensor is proportional to the target gas concentrations (Figure 12d,e) and transmitted using radiofrequency at 405, 433, and 915 MHz. The feasibility of this approach was tested with a CO₂ sensor in four pigs, with two having a high-fiber and two having a low-fiber diet. For pigs with a high-fiber diet, the sensor voltage response decreased significantly between 10 and 18 hours after swallowing the capsule (Figure 12f). This time period corresponds with the digestion time expected for the capsule to reach the small intestine of a pig, and it is in line with the higher levels of CO₂ previously measured in the small intestines of pigs with high-fiber diets compared to those with low-fiber diets. In the future, integration of multiple gas sensors and other capabilities may result in

a disruptive tool for minimally invasive analysis of our digestive system.

5. Summary and Outlook

In conclusion, we have reviewed some recent achievements in miniaturized sensor technologies for the non-invasive, possibly continuous, measurement of important biomarkers for medical diagnostics, healthcare, and lifestyle monitoring. We have proposed a classification according to their application environment, namely body fluid and volatile biomarker sensors. For both categories, the development of flexible electronics is rapidly revolutionizing their layout, allowing the engineering of ultra-thin and compact devices on transferable tattoos and contact lenses. Graphene and carbon fibers have become key components of biocompatible, stretchable electrodes providing improved mechanical properties and adhesion to the substrates. Standing challenges include the power supply and data transmission as well as the development of sufficiently selective and sensitive sensing materials. Highly selective body fluid sensors for readily available sweat, saliva, and tears have been developed leveraging on existing electrochemical biosensor approaches, which can benefit from an extensive library of enzymes for biomolecule detection. Recent progress in the micro-nano fabrication of planar electrochemical cell design has allowed the design of wearable glucose, L-lactate, and ethanol biosensors, with the only apparent limitations being the supply of sufficient voltage for the electrochemical redox reactions and the synthesis of the selective functional groups.

On the other side of the spectrum, volatile biomarker sensors are struggling to achieve the same selectivity of body fluid sensors. They often rely on sensor arrays made of metal oxide and functionalized gold nanoparticles, and pattern recognition approaches to identify specific diseases. Selectivity is also pursued by integration of gas selective membranes, engineering of unique material properties, and strain-induced variation in the morphology of the detector. A strength of volatile biomarker analysis is its intrinsic non-invasive nature that solve some of the strict location and size requirements faced by body fluid sensors. The development of miniaturized fuel cells able to

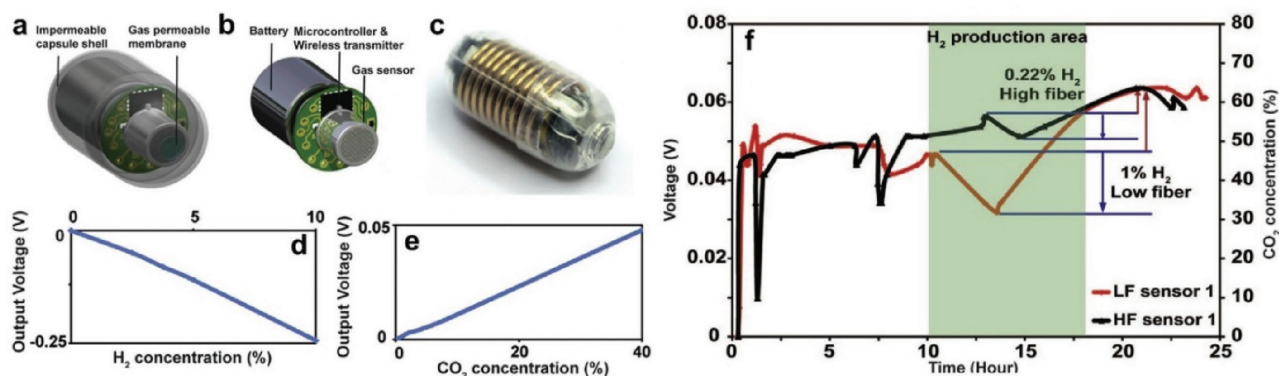


Figure 12. a,b) Schematic layout and c) demonstration of a swallowable gas sensing system consisting of an indigestible and impermeable shell with a gas-permeable membrane; a gas sensor for H₂, CH₄, or CO₂; a microcontroller; a wireless transmitter; and a silver oxide battery. Sensor voltage response to d) H₂ and e) CO₂. f) Measurement of CO₂ in the intestinal system of pig with high- and low-fiber diets.^[12] All panels reproduced with permission.^[12] Copyright 2016, Elsevier.

deliver power from the oxidation of locally available biofuels is a promising emerging concept for the long-term power supply of both body fluid and volatile biomarker sensors. Alternative approaches include the development of passive radio frequency (RF) circuits that are able to provide both the required power for the operation and a convenient means for the data transmission and readout. The size of the required antenna as well as the required proximity of the reader may pose some future limits on the sensor layout, sensor circuit design, and device miniaturization. Nonetheless, optimization of the sensing materials and mechanism for RF operation has only recently begun and is already becoming an enabling tool for the utilization of a multitude of biosensors in difficult-to-wire locations such as the human iris. The future development of wearable and miniaturized sensing technology is bright, with applications in personalized and preventive medicine providing strong social and financial benefits for addressing the large number of standing fundamental and technological challenges.

Acknowledgements

A.T. gratefully acknowledges the support of Australian Research Council DP150101939, Australian Research Council DE160100569 and Westpac2016 Research Fellowship.

Received: October 10, 2016

Revised: December 19, 2016

Published online:

- [1] OECD, *Life Expectancy at Birth*, <https://data.oecd.org/healthstat/life-expectancy-at-birth.htm> (accessed: October 2016).
- [2] a) C. D. Mathers, G. A. Stevens, T. Boerma, R. A. White, M. I. Tobias, *Lancet* **2015**, *385*, 540; b) A. T. C. Collaboration, *Lancet* **2008**, *372*, 293; c) J. Bor, A. J. Herbst, M.-L. Newell, T. Bärnighausen, *Science* **2013**, *339*, 961.
- [3] a) L. Hockaday, K. Kang, N. Colangelo, P. Cheung, B. Duan, E. Malone, J. Wu, L. Girardi, L. Bonassar, H. Lipson, *Biofabrication* **2012**, *4*, 035005; b) B. Leukers, H. Gülkan, S. H. Irsen, S. Milz, C. Tille, M. Schieker, H. Seitz, *J. Mater. Sci. Mater. Med.* **2005**, *16*, 1121.
- [4] a) J. Takacs, C. L. Pollock, J. R. Guenther, M. Bahar, C. Napier, M. A. Hunt, *J. Sci. Med. Sport* **2014**, *17*, 496; b) K. M. Diaz, D. J. Krupka, M. J. Chang, J. Peacock, Y. Ma, J. Goldsmith, J. E. Schwartz, K. W. Davidson, *Int. J. Cardiol.* **2015**, *185*, 138.
- [5] a) K. J. Kim, D.-H. Shin, *Internet Res.* **2015**, *25*, 527; b) A. Carpenter, A. Frontera, *Europace* **2016**, euv427.
- [6] a) J. R. Windmiller, J. Wang, *Electroanalysis* **2013**, *25*, 29; b) A. P. Turner, *Chem. Soc. Rev.* **2013**, *42*, 3184.
- [7] a) M. Navas, A. Jiménez, A. Asuero, *Clin. Chim. Acta* **2012**, *413*, 1171; b) S. N. Rampersad, *Sensors* **2012**, *12*, 12347.
- [8] a) R. M. Gelfand, D. Dey, J. Kohoutek, A. Bonakdar, S. C. Hur, D. Di Carlo, H. Mohseni, *Opt. Photonics News* **2011**, *22*, 32; b) J. T. Kirk, G. E. Fridley, J. W. Chamberlain, E. D. Christensen, M. Hochberg, D. M. Ratner, *Lab Chip* **2011**, *11*, 1372.
- [9] a) A. Agah, K. Vleugels, P. B. Griffin, M. Ronaghi, J. D. Plummer, B. A. Wooley, *IEEE J. Solid-State Circ.* **2010**, *45*, 1099; b) A. S. Sadek, R. B. Karabalin, J. Du, M. L. Roukes, C. Koch, S. C. Masmanidis, *Nano Lett.* **2010**, *10*, 1769.
- [10] M. Righettoni, A. Tricoli, S. Gass, A. Schmid, A. Amann, S. E. Pratsinis, *Anal. Chim. Acta* **2012**, *738*, 69.
- [11] M. X. Chu, K. Miyajima, D. Takahashi, T. Arakawa, K. Sano, S.-i. Sawada, H. Kudo, Y. Iwasaki, K. Akiyoshi, M. Mochizuki, K. Mitsubayashi, *Talanta* **2011**, *83*, 960.
- [12] K. Kalantar-Zadeh, C. K. Yao, K. J. Berean, N. Ha, J. Z. Ou, S. A. Ward, N. Pillai, J. Hill, J. J. Cottrell, F. R. Dunshea, *Gastroenterol.* **2016**, *150*, 37.
- [13] a) A. Sensimed, "White Paper", http://www.sensimed.ch/images/pdf/sensimed_triggerfish_white_paper_2014.pdf (accessed: October 2016); b) Google Press Release, "What is Google doing with a smart contact lens?", <http://www.healthline.com/hlcmsresource/images/diabetesmine/wp-content/uploads/2014/01/Google-Smart-Contacts-One-Pager.pdf> (accessed: October 2016).
- [14] M. S. Mannoor, H. Tao, J. D. Clayton, A. Sengupta, D. L. Kaplan, R. R. Naik, N. Verma, F. G. Omenetto, M. C. McAlpine, *Nature Commun.* **2012**, *3*, 763.
- [15] W. Jia, A. J. Bandodkar, G. Valdés-Ramírez, J. R. Windmiller, Z. Yang, J. Ramírez, G. Chan, J. Wang, *Anal. Chem.* **2013**, *85*, 6553.
- [16] J. Parak, A. Tarniceriu, P. Renevey, M. Bertschi, R. Delgado-Gonzalo, I. Korhonen, presented at 2015 37th Annual International Conference of the IEEE Engineering in Medicine and Biology Society (EMBC), Aug. **2015**.
- [17] M. Righettoni, A. Ragnoni, A. T. Güntner, C. Loccioni, S. E. Pratsinis, T. H. Risby, *J. Breath Res.* **2015**, *9*, 047101.
- [18] Y. Yamada, S. Hiyama, T. Toyooka, S. Takeuchi, K. Itabashi, T. Okubo, H. Tabata, *Anal. Chem.* **2015**, *87*, 7588.
- [19] a) A. D. Association, *Diabetes Care* **2014**, *37*, S81; b) A. D. Association, *P. R. Health Sci. J.* **2013**, *20*, 175.
- [20] S. Gong, W. Schwalb, Y. Wang, Y. Chen, Y. Tang, J. Si, B. Shirinzadeh, W. Cheng, *Nature Commun.* **2014**, *5*, 3132.
- [21] a) A. J. Bandodkar, D. Molinnus, O. Mirza, T. Guinovart, J. R. Windmiller, G. Valdés-Ramírez, F. J. Andrade, M. J. Schöning, J. Wang, *Biosens. Bioelectron.* **2014**, *54*, 603; b) B. Schazmann, D. Morris, C. Slater, S. Beirne, C. Fay, R. Reuveny, N. Moyna, D. Diamond, *Anal. Methods* **2010**, *2*, 342; c) Z. Sonner, E. Wilder, J. Heikenfeld, G. Kasting, F. Beyette, D. Swaile, F. Sherman, J. Joyce, J. Hagen, N. Kelley-Loughnane, R. Naik, *Biomicrofluidics* **2015**, *9*, 031301.
- [22] A. G. Dent, T. G. Sutedja, P. V. Zimmerman, *J. Thorac. Dis.* **2013**, *5*, S540.
- [23] a) A. Manolis, *Clin. Chem.* **1983**, *29*, 5; b) W. Miekisch, J. K. Schubert, G. F. Noeldge-Schomburg, *Clin. Chim. Acta* **2004**, *347*, 25; c) M. Righettoni, A. Amann, S. E. Pratsinis, *Mater. Today* **2015**, *18*, 163.
- [24] S. Patel, H. Park, P. Bonato, L. Chan, M. Rodgers, *J. Neuroeng. Rehabil.* **2012**, *9*, 21.
- [25] N. Hex, C. Bartlett, D. Wright, M. Taylor, D. Varley, *Diabet. Med.* **2012**, *29*, 855.
- [26] a) E. Emmett, *Ann. Clin. Lab. Sci.* **1978**, *8*, 270; b) G. Liu, C. Ho, N. Slappey, Z. Zhou, S. E. Snelgrove, M. Brown, A. Grabinski, X. Guo, Y. Chen, K. Miller, J. Edwards, T. Kaya, *Sens. Actuators, B* **2016**, *227*, 35.
- [27] a) H. Yao, A. J. Shum, M. Cowan, I. Lähdesmäki, B. A. Parviz, *Biosens. Bioelectron.* **2011**, *26*, 3290; b) N. von Thun und Hohenstein-Blaul, S. Funke, F. H. Grus, *Exp. Eye Res.* **2013**, *117*, 126.
- [28] M. Falk, V. Andoralov, M. Silow, M. D. Toscano, S. Shleev, *Anal. Chem.* **2013**, *85*, 6342.
- [29] C. Salvisberg, N. Tajouri, A. Hainard, P. R. Burkhard, P. H. Lalive, N. Turck, *Proteomics Clin. Appl.* **2014**, *8*, 185.
- [30] a) P. Manikis, S. Jankowski, H. Zhang, R. J. Kahn, J.-L. Vincent, *Am. J. Emerg. Med.* **1995**, *13*, 619; b) J. A. Kruse, S. A. J. Zaidi, R. W. Carlson, *Am. J. Med.* **1987**, *83*, 77; c) G. Broder, M. H. Weil, *Science* **1964**, *143*, 1457; d) A. M. Vogt, C. Ackermann, M. Yildiz,

- W. Schoels, W. Kübler, *Biochim. Biophys. Acta, Mol. Basis Dis.* **2002**, 1586, 219; e) B. Phipers, J. T. Pierce, *Br. J. Anaesth.* **2006**, 6, 128.
- [31] T. Yoshida, Y. Suda, N. Takeuchi, *Eur. J. Appl. Physiol.* **1982**, 49, 223.
- [32] a) D. Costill, *Ann. N. Y. Acad. Sci.* **1977**, 301, 160; b) S. Corrie, J. Coffey, J. Islam, K. Markey, M. Kendall, *Analyst* **2015**, 140, 4350.
- [33] H. M. Emrich, E. Stoll, B. Friolet, J. P. Colombo, R. Richterich, E. Rossi, *Pediatr. Res.* **1968**, 2, 464.
- [34] I. Timofeeva, K. Medinskaia, L. Nikolaeva, D. Kirsanov, A. Bulatov, *Talanta* **2016**, 150, 655.
- [35] M. Choudhary, P. Yadav, A. Singh, S. Kaur, J. Ramirez-Vick, P. Chandra, K. Arora, S. P. Singh, *Electroanalysis* **2016**, DOI: 10.1002/elan.201600238n/a.
- [36] S. Kumar, J. G. Sharma, S. Maji, B. D. Malhotra, *Biosens. Bioelectron.* **2016**, 78, 497.
- [37] B. I. Freedman, S. C. Smith, B. M. Bagwell, J. Xu, D. W. Bowden, J. Divers, *Am. J. Nephrol.* **2015**, 41, 438.
- [38] J. Liu, S. Sun, H. Shang, J. Lai, L. Zhang, *Electroanalysis* **2016**, 28, 2016.
- [39] Y. Du, W. Zhang, M. L. Wang, *Biosensors* **2016**, 6, 10.
- [40] T. Arakawa, Y. Kuroki, H. Nitta, K. Toma, K. Mitsubayashi, S. Takeuchi, T. Sekita, S. Minakuchi, presented at *2015 9th International Conference on Sensing Technology (ICST)*, Auckland, New Zealand, December **2015**.
- [41] L. Yu, X. Wei, C. Fang, Y. Tu, *Electrochim. Acta* **2016**, 211, 27.
- [42] A. Roda, M. Guardigli, D. Calabria, M. M. Calabretta, L. Cevenini, E. Michellini, *Analyst* **2014**, 139, 6494.
- [43] C. Timchalk, T. S. Poet, A. A. Kousba, J. A. Campbell, Y. Lin, *J. Toxicol. Environ. Health* **2004**, 67, 635.
- [44] M. Tsunoda, M. Hirayama, T. Tsuda, K. Ohno, *Clin. Chim. Acta* **2015**, 442, 52.
- [45] L. Guo, Y. Wang, Y. Zheng, Z. Huang, Y. Cheng, J. Ye, Q. Chu, D. Huang, *J. Chromatogr. A* **2016**, 1014, 70.
- [46] H. M. Saraoğlu, M. Koçan, *Expert Systems* **2010**, 27, 156.
- [47] C. Liu, Y. Sheng, Y. Sun, J. Feng, S. Wang, J. Zhang, J. Xu, D. Jiang, *Biosens. Bioelectron.* **2015**, 70, 455.
- [48] M. M. Pribil, G. U. Laptev, E. E. Karyakina, A. A. Karyakin, *Anal. Chem.* **2014**, 86, 5215.
- [49] W. C. Mak, K. Y. Cheung, J. Orban, C.-J. Lee, A. P. F. Turner, M. Griffith, *ACS Appl. Mater. Interfaces* **2015**, 7, 25487.
- [50] S. Biagi, S. Ghimenti, M. Onor, E. Bramanti, *Biomed. Chrom.* **2012**, 26, 1408.
- [51] S. Pichini, M. Navarro, R. Pacifici, P. Zuccaro, J. Ortuño, M. Farré, P. N. Roset, J. Segura, R. de la Torre, *J. Anal. Toxicol.* **2003**, 27, 294.
- [52] Y. Hu, X. Jiang, L. Zhang, J. Fan, W. Wu, *Biosens. Bioelectron.* **2013**, 48, 94.
- [53] Q. Yan, B. Peng, G. Su, B. E. Cohan, T. C. Major, M. E. Meyerhoff, *Anal. Chem.* **2011**, 83, 8341.
- [54] K. Karns, A. E. Herr, *Anal. Chem.* **2011**, 83, 8115.
- [55] a) W. V. Giannobile, J. T. McDevitt, R. S. Niedbala, D. Malamud, *Adv. Dent. Res.* **2011**, 23, 375; b) J. Kim, G. Valdes-Ramirez, A. J. Bhandarkar, W. Jia, A. G. Martinez, J. Ramirez, P. Mercier, J. Wang, *Analyst* **2014**, 139, 1632; c) J. Kim, S. Imani, W. R. de Araujo, J. Warchall, G. Valdés-Ramírez, T. R. L. C. Paixão, P. P. Mercier, J. Wang, *Biosens. Bioelectron.* **2015**, 74, 1061.
- [56] H. Graf, H. R. Mühlemann, *Helv. Odontol. Acta* **1966**, 10, 94.
- [57] a) T. Nakagawa, H. Hu, S. Zharikov, K. R. Tuttle, R. A. Short, O. Glushakova, X. Ouyang, D. I. Feig, E. R. Block, J. Herrera-Acosta, J. M. Patel, R. J. Johnson, *Am. J. Physiol. Renal. Physiol.* **2006**, 290, F625; b) G. F. Falasca, *Clin. Dermatol.* **2006**, 24, 498; c) W. L. Nyhan, *J. Inherit. Metab. Dis.* **1997**, 20, 171; d) T. R. Merriman, N. Dalbeth, *Joint Bone Spine* **2011**, 78, 35.
- [58] a) A. Dehghan, M. van Hoek, E. J. G. Sijbrands, A. Hofman, J. C. M. Witteman, *Diabetes Care* **2008**, 31, 361; b) M. Zloczower, A. Z. Reznick, R. O. Zouby, R. M. Nagler, *Antioxid. Redox Signal.* **2007**, 9, 765; c) A. Costa, I. Igualá, J. Bedini, L. Quintó, I. Conget, *Metabolism* **2002**, 51, 372; d) V. Bhole, J. W. J. Choi, S. Woo Kim, M. De Vera, H. Choi, *Am. J. Med.* **2010**, 123, 957.
- [59] a) Y. Hellsten, P. C. Tullson, E. A. Richter, J. Bangsbo, *Free Radic. Biol. Med.* **1997**, 22, 169; b) B. Owen-Smith, J. Quiney, J. Read, *Lancet* **1998**, 351, 1932.
- [60] K. Shibasaki, M. Kimura, R. Ikarashi, A. Yamaguchi, T. Watanabe, *Metabolomics* **2012**, 8, 484.
- [61] M. Soukup, I. Biesiada, A. Henderson, B. Idowu, D. Rodeback, L. Ridpath, E. G. Bridges, A. M. Nazar, K. G. Bridges, *Diabetol. Metab. Syndr.* **2012**, 4, 1.
- [62] F. D. Shah, R. Begum, B. N. Vajaria, K. R. Patel, J. B. Patel, S. N. Shukla, P. S. Patel, *Indian J. Clin. Biochem.* **2011**, 26, 326.
- [63] J. M. Turner-Cobb, S. E. Sephton, C. Koopman, J. Blake-Mortimer, D. Spiegel, *Psychosom. Med.* **2000**, 62, 337.
- [64] S. Mi, J. Lu, M. Sun, Z. Li, H. Zhang, M. B. Neilly, Y. Wang, Z. Qian, J. Jin, Y. Zhang, S. K. Bohlander, M. M. Le Beau, R. A. Larson, T. R. Golub, J. D. Rowley, J. Chen, *Proc. Natl. Acad. Sci. USA* **2007**, 104, 19971.
- [65] W.-S. Wang, W.-T. Kuo, H.-Y. Huang, C.-H. Luo, *Sensors* **2010**, 10, 1782.
- [66] S. Azouz, L. Rotariu, A. M. Benito, W. K. Maser, M. B. Ali, C. Bala, *Biosens. Bioelectron.* **2015**, 69, 280.
- [67] P. Bollella, G. Fusco, C. Tortolini, G. Sanzò, G. Favero, L. Gorton, R. Antiochia, *Biosens. Bioelectron.* **2016**, 89, 152.
- [68] a) M. J. Whitcombe, I. Chianella, L. Larcombe, S. A. Piletsky, J. Noble, R. Porter, A. Horgan, *Chem. Soc. Rev.* **2011**, 40, 1547; b) G.-Z. Chen, I.-S. Chan, D. C. C. Lam, *Sens. Actuators, A* **2013**, 203, 112.
- [69] N. Thomas, I. Lähdesmäki, B. A. Parviz, *Sens. Actuators, B* **2012**, 162, 128.
- [70] Y. T. Liao, H. Yao, A. Lingley, B. Parviz, B. P. Otis, *IEEE J. Solid-State Circ.* **2012**, 47, 335.
- [71] N. M. Farandos, A. K. Yetisen, M. J. Monteiro, C. R. Lowe, S. H. Yun, *Adv. Healthcare Mater.* **2015**, 4, 792.
- [72] H. Yao, Y. Liao, A. Lingley, A. Afanasiev, I. Lähdesmäki, B. Otis, B. Parviz, *J. Micromech. Microeng.* **2012**, 22, 075007.
- [73] J. T. Baca, C. R. Taormina, E. Feingold, D. N. Finegold, J. J. Grabowski, S. A. Asher, *Clin. Chem.* **2007**, 53, 1370.
- [74] a) M. Falk, V. Andoralov, Z. Blum, J. Sotres, D. B. Suyatin, T. Ruzgas, T. Arnebrant, S. Shleev, *Biosens. Bioelectron.* **2012**, 37, 38; b) M. Falk, Z. Blum, S. Shleev, *Electrochim. Acta* **2012**, 82, 191.
- [75] V. Baeyens, R. Gurny, *Pharm. Acta Helv.* **1997**, 72, 191.
- [76] C. Zuliani, G. Matzeu, D. Diamond, *Electrochim. Acta* **2014**, 132, 292.
- [77] R. S. Malon, S. Sadir, M. Balakrishnan, E. P. Córcoles, *BioMed Res. Int.* **2014**, 2014, 962903.
- [78] C. Lee, X. Wei, J. W. Kysar, J. Hone, *Science* **2008**, 321, 385.
- [79] S. P. Koenig, N. G. Boddeti, M. L. Dunn, J. S. Bunch, *Nature Nanotechnol.* **2011**, 6, 543.
- [80] a) C. Chen, S. Rosenblatt, K. I. Bolotin, W. Kalb, P. Kim, I. Kymissis, H. L. Stormer, T. F. Heinz, J. Hone, *Nature Nanotechnol.* **2009**, 4, 861; b) L. Liao, Y.-C. Lin, M. Bao, R. Cheng, J. Bai, Y. Liu, Y. Qu, K. L. Wang, Y. Huang, X. Duan, *Nature* **2010**, 467, 305; c) Y. Liu, D. Yu, C. Zeng, Z. Miao, L. Dai, *Langmuir* **2010**, 26, 6158.
- [81] G. Matzeu, L. Florea, D. Diamond, *Sens. Actuators, B* **2015**, 211, 403.
- [82] J. Kim, I. Jeeran, S. Imani, T. N. Cho, A. Bhandarkar, S. Cinti, P. P. Mercier, J. Wang, *ACS Sensors* **2016**, 1, 1011.
- [83] R. S. Hubbard, *J. Biol. Chem.* **1920**, 43, 57.
- [84] a) D. J. Kearney, T. Hubbard, D. Putnam, *Dig. Dis. Sci.* **2002**, 47, 2523; b) S. Suerbaum, P. Michetti, *N. Engl. J. Med.* **2002**, 347, 1175.
- [85] A. D. Smith, J. O. Cowan, K. P. Brassett, G. P. Herbison, D. R. Taylor, *N. Engl. J. Med.* **2005**, 352, 2163.

- [86] a) H. Haick, Y. Y. Broza, P. Mochalski, V. Ruzsanyi, A. Amann, *Chem. Soc. Rev.* **2014**, *43*, 1423; b) A. Anton, M. Pawel, R. Vera, Y. B. Yoav, H. Hossam, *J. Breath Res.* **2014**, *8*, 016003; c) Y. Y. Broza, H. Haick, *Nanomedicine* **2013**, *8*, 785.
- [87] a) C. Deng, X. Zhang, N. Li, *J. Chromatogr. B* **2004**, *808*, 269; b) R. Xue, L. Dong, S. Zhang, C. Deng, T. Liu, J. Wang, X. Shen, *Rapid Commun. Mass Spectrom.* **2008**, *22*, 1181.
- [88] a) O. Barash, W. Zhang, J. M. Halpern, Q. L. Hua, Y. Y. Pan, H. Kayal, K. Khoury, H. Liu, M. P. A. Davies, H. Haick, *Oncotarget* **2015**, *6*, 44864; b) C. Brunner, W. Szymczak, V. Höllriegl, S. Mörtl, H. Oelmez, A. Bergner, R. M. Huber, C. Hoeschen, U. Oeh, *Anal. Bioanal. Chem.* **2010**, *397*, 2315; c) P. Mochalski, A. Sponring, J. King, K. Unterkofler, J. Troppmair, A. Amann, *Cancer Cell Int.* **2013**, *13*, 1.
- [89] a) W. B. Agnes, J. B. N. v. B. Joep, W. D. Jan, S. Agnieszka, F. W. Emile, J. v. S. Frederik, *J. Breath Res.* **2012**, *6*, 027108; b) A. Amann, M. Corradi, P. Mazzone, A. Mutti, *Expert Rev. Mol. Diagn.* **2011**, *11*, 207.
- [90] a) A. D'Amico, R. Bono, G. Pennazza, M. Santonico, G. Mantini, M. Bernabei, M. Zarlenga, C. Roscioni, E. Martinelli, R. Paolesse, C. Di Natale, *Skin Res. Technol.* **2008**, *14*, 226; b) G. Pennazza, M. Santonico, E. Martinelli, R. Paolesse, V. Tamburrelli, S. Cristina, A. D'Amico, C. Di Natale, A. Bartolazzi, *Sens. Actuators, B* **2011**, *154*, 288; c) A. N. Thomas, S. Riazanskaia, W. Cheung, Y. Xu, R. Goodacre, C. L. P. Thomas, M. S. Baguneid, A. Bayat, *Wound Repair Regen.* **2010**, *18*, 391.
- [91] a) B. D. L. Costello, R. Ewen, A. K. Ewer, C. E. Garner, C. S. J. Probert, N. M. Ratcliffe, S. Smith, *J. Breath Res.* **2008**, *2*, 037023; b) T. G. de Meij, I. B. Larbi, M. P. van der Schee, Y. E. Lentferink, T. Paff, J. S. Terhaar sive Droste, C. J. Mulder, A. A. van Bodegraven, N. K. de Boer, *Int. J. Cancer* **2014**, *134*, 1132; c) M. K. Bomers, F. P. Menke, R. S. Savage, C. M. J. E. Vandenbroucke- Grauls, M. A. van Agtmael, J. A. Covington, Y. M. Smulders, *Am. J. Gastroenterol.* **2015**, *110*, 588.
- [92] a) Y. Hanai, K. Shimono, K. Matsumura, A. Vachani, S. Albelda, K. Yamazaki, G. K. Beauchamp, H. Oka, *Biosci. Biotechnol. Biochem.* **2012**, *76*, 679; b) K. M. Banday, K. K. Pasikanti, E. C. Y. Chan, R. Singla, K. V. S. Rao, V. S. Chauhan, R. K. Nanda, *Anal. Chem.* **2011**, *83*, 5526; c) K. U. Alwis, B. C. Blount, A. S. Britt, D. Patel, D. L. Ashley, *Anal. Chim. Acta* **2012**, *750*, 152.
- [93] T. Pfafe, J. Cooper-White, P. Beyerlein, K. Kostner, C. Punyadeera, *Clin. Chem.* **2011**, *57*, 675.
- [94] a) S. R. Kim, R. U. Halden, T. J. Buckley, *Environ. Sci. Technol.* **2007**, *41*, 1662; b) J. Fisher, D. Mahle, L. Bankston, R. Greene, J. Gearhart, *Am. Ind. Hyg. Assoc. J.* **1997**, *58*, 425.
- [95] a) B. d. L. Costello, A. Amann, H. Al-Kateb, C. Flynn, W. Filipiak, T. Khalid, D. Osborne, N. M. Ratcliffe, *J. Breath Res.* **2014**, *8*, 014001; b) A. Amann, W. Miekisch, J. Schubert, B. Buszewski, T. Ligor, T. Jezierski, J. Pleil, T. Risby, *Annu. Rev. Anal. Chem.* **2014**, *7*, 455.
- [96] M. Shirasu, K. Touhara, *J. Biochem.* **2011**, *150*, 257.
- [97] a) A. Tricoli, M. Righettoni, A. Teleki, *Angew. Chem., Int. Ed.* **2010**, *49*, 7632; b) R. Marco, T. Antonio, *J. Breath Res.* **2011**, *5*, 037109.
- [98] a) I. Kusch, B. Arendacká, S. Štolc, P. Mochalski, W. Filipiak, K. Schwarz, L. Schwentner, A. Schmid, A. Dzien, M. Lechleitner, *Clin. Chem. Lab. Med.* **2008**, *46*, 1011; b) M. Basanta, R. M. Jarvis, Y. Xu, G. Blackburn, R. Tal-Singer, A. Woodcock, D. Singh, R. Goodacre, C. P. Thomas, S. J. Fowler, *Analyst* **2010**, *135*, 315.
- [99] Y.-H. Yun, E. Eteshola, A. Bhattacharya, Z. Dong, J.-S. Shim, L. Conforti, D. Kim, M. Schulz, C. Ahn, N. Watts, *Sensors* **2009**, *9*, 9275.
- [100] a) A. T. Güntner, V. Koren, K. Chikkadi, M. Righettoni, S. E. Pratsinis, *ACS Sensors* **2016**, *1*, 528; b) M. Righettoni, A. Tricoli, S. E. Pratsinis, *Anal. Chem.* **2010**, *82*, 3581.
- [101] H. G. Moon, Y.-S. Shim, D. H. Kim, H. Y. Jeong, M. Jeong, J. Y. Jung, S. M. Han, J. K. Kim, J.-S. Kim, H.-H. Park, J.-H. Lee, H. L. Tuller, S.-J. Yoon, H. W. Jang, *Sci. Rep.* **2012**, *2*, 588.
- [102] a) R. Arsat, M. Breedon, M. Shafiei, P. G. Spizziri, S. Gilje, R. B. Kaner, K. Kalantar-zadeh, W. Wlodarski, *Chem. Phys. Lett.* **2009**, *467*, 344; b) M. K. Kurosawa, *Ultrasonics* **2000**, *38*, 15.
- [103] A. Tricoli, S. E. Pratsinis, *Nature Nanotechnol.* **2010**, *5*, 54.
- [104] P. Gouma, K. Kalyanasundaram, X. Yun, M. Stanacevic, L. Wang, *IEEE Sens. J.* **2010**, *10*, 49.
- [105] C. Sun, P. K. Dutta, *Sens. Actuators, B* **2016**, *226*, 156.
- [106] Y.-C. Weng, Y.-H. Yang, I.-T. Lu, *J. Nanosci. Nanotechnol.* **2016**, *16*, 7077.
- [107] Y.-K. Cheng, C.-H. Lin, T. Kaneta, T. Imasaka, *J. Chromatogr. A* **2010**, *1217*, 5274.
- [108] H. G. Moon, Y. Jung, S. D. Han, Y.-S. Shim, B. Shin, T. Lee, J.-S. Kim, S. Lee, S. C. Jun, H.-H. Park, C. Kim, C.-Y. Kang, *ACS Appl. Mater. Interfaces* **2016**, *8*, 20969.
- [109] L. M. Heaney, D. M. Ruskiewicz, K. L. Arthur, A. Hadjithekli, C. Aldcroft, M. R. Lindley, C. P. Thomas, M. A. Turner, J. C. Reynolds, *Bioanalysis* **2016**, *8*, 1325.
- [110] N. Kahn, O. Lavie, M. Paz, Y. Segev, H. Haick, *Nano Lett.* **2015**, *15*, 7023.
- [111] B. Grabowska-Polanowska, J. Faber, M. Skowron, P. Miarka, A. Pietrzycka, I. Śliwka, A. Amann, *J. Chromatogr. A* **2013**, *1301*, 179.
- [112] M. Chatterjee, X. Ge, Y. Kostov, P. Luu, L. Tolosa, H. Woo, R. Viscardi, S. Falk, R. Potts, G. Rao, *Physiol. Meas.* **2015**, *36*, 883.
- [113] J. Park, J. Kim, K. Kim, S.-Y. Kim, W. H. Cheong, K. Park, J. H. Song, G. Namgoong, J. J. Kim, J. Heo, F. Bien, J.-U. Park, *Nanoscale* **2016**, *8*, 10591.
- [114] S. M. Cristescu, R. Berkelmans, S. te Lintel Hekkert, B. H. Timmerman, D. H. Parker, F. J. Harren, *Proc. SPIE* **2000**, *4162*, DOI 10.1117/12.405929.
- [115] M. A. Pleitez, T. Lieblein, A. Bauer, O. Hertzberg, H. von Lilienfeld-Toal, W. Mäntele, *Anal. Chem.* **2013**, *85*, 1013.
- [116] P. Lundin, E. K. Svanberg, L. Coccola, M. L. Xu, G. Somesfalean, S. Andersson-Engels, J. Jahr, V. Fellman, K. Svanberg, S. Svanberg, *BIOMEDO* **2013**, *18*, 127005.
- [117] Z. H. Ibutopo, S. M. U. A. Shah, K. Khun, M. Willander, *Sensors* **2012**, *12*, 2456.
- [118] A. Ikeda, S. Nishiumi, M. Shinohara, T. Yoshie, N. Hatano, T. Okuno, T. Bamba, E. Fukusaki, T. Takenawa, T. Azuma, M. Yoshida, *Biomed. Chrom.* **2012**, *26*, 548.
- [119] M. Yoshida, N. Hatano, S. Nishiumi, Y. Irino, Y. Izumi, T. Takenawa, T. Azuma, *J. Gastroenterol.* **2012**, *47*, 9.
- [120] Z.-M. Liu, L. Feng, J. Hou, X. Lv, J. Ning, G.-B. Ge, K.-W. Wang, J.-N. Cui, L. Yang, *Sens. Actuators, B* **2014**, *205*, 151.
- [121] W. Dai, M. Li, H. Li, B. Yang, *Sens. Actuators, B* **2014**, *201*, 31.
- [122] M. Puiui, A.-M. Gurban, L. Rotariu, S. Brajnicov, C. Viespe, C. Bala, *Sensors* **2015**, *15*, 10511.
- [123] D. D. Deobagkar, V. Limaye, S. Sinha, R. D. S. Yadava, *Sens. Actuators, B* **2005**, *104*, 85.
- [124] Y. Chang, N. Tang, H. Qu, J. Liu, D. Zhang, H. Zhang, W. Pang, X. Duan, *Sci. Rep.* **2016**, *6*, 23970.
- [125] S.-t. He, Y.-b. Gao, J.-y. Shao, Y.-y. Lu, *Proc. SPIE* **2000**, *4162*, 101.
- [126] T. L. Panasyuk, V. M. Mirsky, S. A. Piletsky, O. S. Wolfbeis, *Anal. Chem.* **1999**, *71*, 4609.
- [127] G. Peng, U. Tisch, O. Adams, M. Hakim, N. Shehada, Y. Y. Broza, S. Billan, R. Abdah-Bortnyak, A. Kuten, H. Haick, *Nature Nanotechnol.* **2009**, *4*, 669.
- [128] M. K. Nakhleh, S. Baram, R. Jeries, R. Salim, H. Haick, M. Hakim, *Adv. Mater. Technol.* **2016**, *1*, DOI:10.1002/admt.201600132.
- [129] M. Righettoni, A. Tricoli, S. E. Pratsinis, *Chem. Mater.* **2010**, *22*, 3152.

- [130] A. Tricoli, M. Graf, F. Mayer, S. Kühne, A. Hierlemann, S. E. Pratsinis, *Adv. Mater.* **2008**, *20*, 3005.
- [131] a) J. Zhang, X. Liu, G. Neri, N. Pinna, *Adv. Mater.* **2016**, *28*, 795;
b) A. Arena, N. Donato, G. Saitta, A. Bonavita, G. Rizzo, G. Neri, *Sens. Actuators, B* **2010**, *145*, 488.
- [132] B. P. J. d. L. Costello, R. J. Ewen, N. M. Ratcliffe, M. Richards, *J. Breath Res.* **2008**, *2*, 037017.
- [133] M. Epifani, E. Comini, P. Siciliano, G. Faglia, J. R. Morante, *Sens. Actuators, B* **2015**, *217*, 193.
- [134] N. Nasiri, R. Bo, F. Wang, L. Fu, A. Tricoli, *Adv. Mater.* **2015**, *27*, 4336.
- [135] T. Shi, D. Li, Y. Ji, G. Li, K. Xu, *Proc. SPIE* **2012**, 8215, DOI: 10.1117/12.907733.
- [136] S. B. Menees, H. M. Kim, E. E. Elliott, J. L. Mickevicius, B. B. Graustein, P. S. Schoenfeld, *Gastrointest. Endosc.* **2013**, *78*, 510.
- [137] J. L. Toennies, G. Tortora, M. Simi, P. Valdastris, R. J. Webster, *Inst. Mech. Eng. C.J. Mech. Eng. Sci.* **2010**, *224*, 1397.
-